ELECTROMAGNETIC METHODS IN APPLIED GEOPHYSICS—APPLICATIONS
Part A

INTRODUCTION

Misac N. Nabighian

Electromagnetic Methods in Applied Geophysics, Volume I, Theory presented the mathematical and physical foundations common to all EM methods. The purpose of Volume I was to help facilitate the understanding of the theory involved and to provide a limited amount of interpretational aids. *Volume II, Applications* is devoted to a method-by-method treatment of the principal EM techniques in common use.

The first chapter gives a unified treatment of the physical basis of EM methods of exploration and is followed by a comprehensive chapter on the magnetometric resistivity method (MMR). The inclusion of MMR, essentially a dc technique, in an EM volume might seem puzzling at first. However, an increased understanding of current channeling (current gathering, galvanic) effects indicates that anomalies attributable to current channeling can be interpreted best using MMR concepts. In many instances, EM induction plays only a small part in the observed anomaly which is predominantly attributable to current channeling. A case in point is the VLF technique. Not long ago all interpretation was done using only EM induction concepts. Today, some geophysicists describe VLF as "MMR with phase", a tacit acknowledgment of the important role played by current channeling effects in observed VLF anomalies.

The following chapters give in depth treatments of:

Profiling methods using small sources,
Large-layout harmonic field systems,
Electromagnetic soundings,
Time domain electromagnetic prospecting methods,
Geological mapping using VLF radio fields,
The magnetotelluric methods,
Controlled source audio-frequency magnetotellurics,
Airborne electromagnetic methods,
Drillhole EM techniques, and
Electrical exploration methods for the seafloor.

Each chapter describes in detail a given EM method, from instrumentation and field procedures to data interpretation and case histories. Where there were competing field instruments or techniques, a deliberate effort was made to achieve a balance between sometimes divergent claims. To this end, each chapter has an abundance of case histories illustrating various viewpoints.

Except for the common theoretical background which was outlined in the first volume, each chapter is self contained. Special attention was given to eliminating as much as possible duplication between various chapters and to obtaining a certain uniformity in presentation. The large number of topics covered necessitates dividing this second volume into two parts. The twelve chapters are arbitrarily divided into Part A and Part B.

A large portion of the material has never before been published in a systematic way in the western scientific literature. Volume II presents an up-to-date treatment of EM methods that should prove invaluable both to exploration geophysicists (mining, petroleum, environmental, etc.) and to university students studying applied geophysics or related sciences.

Three years have passed since the publication of Volume I—longer than was initially anticipated. With gratitude I acknowledge the continuous support from Jack Corbett, Project Editor, from Dr. Stan Ward, and from the Society of Exploration Geophysicists. The authors contributed greatly by the additional rewriting and updating of their manuscripts to provide state-of-the-art information. Considering the rate at which new developments are being published each year, this was no easy task and I am grateful for their efforts. Last, but definitely not least, my sincerest thanks go to the SEG Publication staff (Lynn Griffin, Jerry Henry, and John Hyden) who patiently survived missed deadlines, multiple updates of various chapters, and frequent changes in book format. Their professionalism was indeed remarkable. Without their help this book would not have been possible.

CHAPTER 1

PHYSICS OF THE ELECTROMAGNETIC INDUCTION EXPLORATION METHOD

G. F. West and J. C. Macnae‡*

INTRODUCTION

The immediate objective of a geophysical survey is to obtain some information about the interior spatial distribution of one or more of the earth's physical properties from a limited set of measurements of a related physical field made on the earth's surface (or another accessible place). In the case of an electromagnetic (EM) induction survey, the most relevant physical property is the electrical conductivity, and it is sensed by means of a time-varying magnetic and/or electric field. The procedure of converting field measurements to a physical property distribution is termed modeling or interpretation, and the formal corresponding mathematical process is termed inversion.

Geophysical inversion is difficult in the best of circumstances because of numerous intrinsic ambiguities. For EM methods in particular there is an additional problem. The basic laws that relate the EM field to the physical property distribution are well known (Maxwell's equations) and a quantitative and calculable relationship between the physical measurements and the property structure can be established for certain idealized cases. However, we still lack practicable modeling capabilities that enable quantitative prediction of the EM field configuration produced by an arbitrary physical property distribution of even moderate complexity.

Geologic scenarios are extremely varied, and few actual cases can be described accurately in terms of simple geometric forms like plane horizontal layers. Thus, only rarely can we feasibly turn geophysical observations directly into a reliable picture of earth structure simply by application of an automatic process. Generally, a human interpreter is still needed to guide the interpretation process, and this human needs to have a good qualitative understanding of how physical earth structure can interact with EM fields. In addition the interpreter should be able to mentally extrapolate beyond calculable cases and to select more important features of the data from less important ones. Our objective in this tutorial paper is to assist readers in developing such an ability by discussing the various physical processes which arise in some simple situations.

Mental modeling of electromagnetic methods can be difficult. Unlike gravity and magnetic methods where most geophysicists can sketch with a fair degree of accuracy the potential field configuration around a given susceptibility or density distribution, the survey results of EM methods seem often to resist visualization in terms of the physical processes in the ground which produce them. One reason is the need to consider two vector fields simultaneously (electric and magnetic). Another is that the EM response is rate dependent. A third reason is that (as in seismic methods) the EM field is usually generated locally by a controlled source which is moved frequently during the survey, so often only one or a few measurements are made of the physical field before changing it. Furthermore, low-frequency diffusive EM field propagation is often more difficult to describe than high-frequency wave propagation where Snell's law ray theory offers a simple first approximation picture that anyone can understand.

Although the mathematical theory of EM fields is an essential tool for EM modeling, focusing too intently on the mathematical niceties can distract the interpreter from the essential physics. Also, description of

*Geophysics Laboratory, Department of Physics, University of Toronto, Toronto, Canada, M5S-1A7.
‡Lamontagne Geophysics Limited, 4A Whiting Street, Artarmon, New South Wales 2064, Australia.

low-frequency EM induction by use of convenient mathematical analogies with wave theory can obscure the fact that eddy current induction at low frequency has more in common with potential field processes such as gravity and magnetics and diffusive processes like conduction of heat and with the widely understood properties of L, R, C electric circuits than it has with high-frequency wave processes epitomized by optical ray theory. Throughout this chapter we have chosen to draw out the electric engineering analogy of L, R, C circuit waveform analysis whose jargon is based on that usually used in the analysis of mathematical functions of complex variables. For readers without a background in complex variables or circuit design, the descriptions of time-domain behavior may be more easily understood.

Because this is a tutorial rather than a review paper, no attempt was made to cite all the significant contributions made during development of the field by very many scientists and engineers. The references given are to convenient sources of additional information and to the sources of specific data. Most examples shown are from work performed at the University of Toronto. The mathematical theory of EM induction is thoroughly reviewed in EM Volume 1, Ward and Hohmann. To define terms, and to provide a brief revision of the basic physics, a short review of elementary principles is given in the first two sections.

BASIC PRINCIPLES

The EM field has two directly measureable components, the electric and magnetic fields. In free space, the two fields can be described equally well either in terms of the field intensity vectors **E** (V/m) and **H** (A/m) or the flux density vectors **D** (C/m^2) and **B** (Wb/m^2 = teslas). These fields are, in general, functions of spatial position (**r**; x, y, z) and also of time t (seconds) or frequency f (hertz) (or angular frequency $\omega = 2\pi f$). Inside a medium where the physical properties vary from point to point usually both the field intensities and the fluxes must be known. Alternatively, if all the magnetizations and electric polarizations created in the medium are known, only one electric and one magnetic vector is required for a full description. Since most geophysicists are quite familiar with the force fields **E** and **H** of static potential theory, we describe the field mainly in terms of **E** and **H**.

At the most fundamental level, the EM field is a

TABLE OF SYMBOLS

a	dimension
A	inductive limit
B	magnetic flux density
c	free constant
D	electric flux density
e	emf
E	electric field intensity
G	Greens function
h	overburden thickness
H	magnetic field intensity
i	$\sqrt{-1}$
I	current
j	electric dipole moment
J	current density
k	wave number
l	horizontal scale parameter
L	inductance
$\underset{\sim}{\mathbf{L}}$	inductance matrix
m	magnetic dipole moment
M	magnetization
N	depolarization factor
P	electric polarization
q	charge density
r	spherical radius
R	resistance
R_0	response of overburden
R	resistance matrix
$\tilde{s}$	thickness
$\underset{\sim}{\mathbf{S}}$	diagonal matrix
t	time
T_0	overburden transmission filter
$u(t)$	step function
U	distribution of magnetization
$\underset{\sim}{\mathbf{U}}$	eigenvector matrix
$\tilde{V}$	volume
x, y, z	cartesian coordinates
$\underset{\sim}{\mathbf{Z}}$	impedance matrix
α	current channeling number
β	half-space response parameter
γ	inductive response parameter
δ	skin depth
$\delta(t)$	delta function
ε	dielectric permittivity
ε_0	dielectric permittivity of free space
η	admittivity
θ	spherical coordinate
κ_ε	dielectric susceptibility
κ_μ	magnetic susceptibility
κ_σ	relative ohmic susceptibility
λ	spatial wavelength
Λ	propagation wavelength
μ	magnetic permeability
μ_0	magnetic permeability of free space
ρ	cylindrical coordinate radius
σ	conductivity
τ	time constant
ϕ	spherical coordinate
Φ	flux
ω	angular frequency

Subscripts and Superscripts

X_a	anomalous
X_b	body
X_c	conduction
X_h	halfspace
X_i, X_j	index
X_o	overburden (except ε_0, μ_0)
X_r	receiver
X_t	transmitter
X_T	total
X^E	electric field
X^H	magnetic field
X^j	electric dipole source
X^m	magnetic dipole source
X^p	primary
X^s	secondary
X'	source

manifestation of the distribution of electric charge. The most direct expression of this electric charge is the Coulomb Law, which in differential form is

$$\nabla \cdot \varepsilon_0 \mathbf{E} = q, \tag{1}$$

i.e., the electric field in free space diverges from any distribution of charge q (C/m^3).

Charge generates another type of field when it moves. This type of field arises in isolation from the static electric field whenever there is a differential flow of charges of opposite sign; a flow wherein the net charge density remains zero. Free electric charge can move at the macroscopic level in nature as free electrons (or electron deficiencies in a crystal lattice) or as mobile ions, and can also circulate widely inside a conductive medium without affecting the overall charge balance in the interior of the medium. Neutral current flow is described by the electric current flux density vector $\mathbf{J}$ (A/m^2) and, as shown in the following discussion, generates a magnetic field which circulates around $\mathbf{J}$ according to Ampere's law. Since charges cannot be created or destroyed, $\mathbf{J}$ must also satisfy a charge conservation constraint

$$\nabla \cdot \mathbf{J} = -\frac{\partial q}{\partial t}. \tag{2}$$

The density of current which flows in a material medium as the result of the electric field usually depends linearly on the electric field strength according to Ohm's law,

$$\mathbf{J} = \sigma \mathbf{E}, \tag{3}$$

where the proportionality constant σ is a property of the material known as the electrical conductivity (S/m).

Microscopic local imbalances in charge distribution and local current circulations at the atomic level in a material medium can create macroscopic EM fields. Electric and magnetic polarization vectors $\mathbf{P}$ and $\mathbf{M}$ describe these effects. ($\mathbf{M}$ is usually called just the magnetization.) In differential form the source relations are

$$\nabla \cdot \varepsilon_0 \mathbf{E} = -\nabla \cdot \mathbf{P}$$

and

$$\nabla \cdot \mathbf{H} = -\nabla \cdot \mathbf{M}. \tag{4}$$

Whereas charge appears in the Coulomb law as a pole source, the polarization vectors act as source dipoles. The relationships are sketched in Figure 1.

In many media, the polarizations are themselves created by the fields, according to linear proportionalities

$$\mathbf{P} = \kappa_\varepsilon \varepsilon_0 \mathbf{E}$$

and

$$\mathbf{M} = \kappa_\mu \mathbf{H}, \tag{5}$$

where κ_ε is called the dielectric susceptibility and κ_μ the magnetic susceptibility of the medium. The defining relationships between the flux density and the intensity vectors are just

$$\mathbf{D} = \varepsilon_0 \mathbf{E} + \mathbf{P}$$

and

$$\mathbf{B} = \mu_0(\mathbf{H} + \mathbf{M}). \tag{6}$$

Separating those polarizations and currents which are induced directly in the medium by the EM field from other source distributions is often necessary. The terms "source distribution" (denoted by a primed symbol), refers to any spatial distribution of $\mathbf{M}$, $\mathbf{P}$, or $\mathbf{J}$ which is independent of the $\mathbf{E}$ and $\mathbf{H}$ fields that are under consideration. A "source" is usually supported by some external energy source. Collecting all the above relationships, we have

$$\mathbf{D} = \varepsilon_0 \mathbf{E} + \mathbf{P} + \mathbf{P}' = \varepsilon \mathbf{E} + \mathbf{P}',$$

where

$$\varepsilon = \varepsilon_0(1 + \kappa_\varepsilon), \tag{7}$$

$$\mathbf{B} = \mu_0(\mathbf{H} + \mathbf{M} + \mathbf{M}') = \mu \mathbf{H} + \mu_0 \mathbf{M}',$$

where

$$\mu = \mu_0(1 + \kappa_\mu), \tag{8}$$

$$\mathbf{J} = \mathbf{J}_c + \mathbf{J}' = \sigma \mathbf{E} + \mathbf{J}', \tag{9}$$

and where $\mathbf{J}_c$ is the ohmic conduction current. Combining the above we obtain

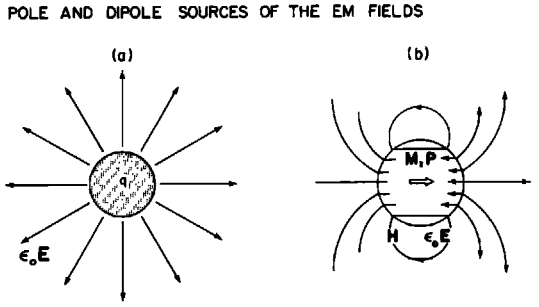

Fig. 1. Configuration of the EM field near pole (a) and dipole (b) source distributions. Note that the $\mathbf{M}$ and $\mathbf{P}$ source dipoles are opposite in direction to the internal field.

$$\nabla \cdot \varepsilon_0 \mathbf{E} = q - \nabla \cdot (\mathbf{P} + \mathbf{P}'),$$

$$\nabla \cdot \mathbf{J} = -\frac{\partial q}{\partial t},$$

and

$$\nabla \cdot \mathbf{H} = -\nabla(\mathbf{M} + \mathbf{M}'). \quad (10)$$

The first two of these equations are closely related. Writing both equations in terms of the electric field, we see that

$$\nabla \cdot (\sigma \mathbf{E} + \varepsilon \partial \mathbf{E}/\partial t) = -\nabla \cdot (\mathbf{J}' + \partial \mathbf{P}'/\partial t) \quad (11)$$

which can be solved to show that if a source distribution is suddenly established in a uniform medium, the electric field will equilibrate exponentially as $e^{-\sigma t/\varepsilon}$. The time constant ε/σ is negligible in most cases, being less than 1 μs in a medium whose conductivity is greater than about 20 μS/m (or resistivity less than 50 000 Ω-m). Thus, for low-frequency EM exploration problems, the only charge and polarization that is important in creating a sustained electric field is that which is maintained by a flux density of source current, i.e.,

$$\nabla \cdot \sigma \mathbf{E} = -\nabla \cdot \mathbf{J}'. \quad (12)$$

The divergence equations (10) have a simpler form when they are written in terms of the total flux density vectors, i.e.,

$$\nabla \cdot \mathbf{D} = q,$$

$$\nabla \cdot \mathbf{J} = -\frac{\partial q}{\partial t},$$

and

$$\nabla \cdot \mathbf{B} = 0, \quad (13)$$

which in a conductive region becomes

$$\nabla \cdot \mathbf{J} = 0,$$

and

$$\nabla \cdot \mathbf{B} = 0. \quad (14)$$

Coupling between the **E** and **H** fields is described by Ampere's and Faraday's laws. Each field generates a component of the other in the form of a circulation about its field lines, as sketched in Figure 2. An electric field is created circulating about any time-varying magnetic field, and a magnetic field is created circulating about any time-varying electric field or electric current density.

$$\nabla \times \mathbf{E} = -\frac{\partial \mathbf{B}}{\partial t},$$

and

$$\nabla \times \mathbf{H} = \frac{\partial \mathbf{D}}{\partial t} + \mathbf{J}. \quad (15)$$

It is a useful shorthand to say that the magnetic field is generated by a *total* current $\mathbf{J}_T$ which is the sum of the ohmic current flow and the so-called *displacement current* $\partial \mathbf{D}/\partial t$.

$$\nabla \times \mathbf{H} = \mathbf{J}_T. \quad (16)$$

This concept is most useful in the frequency domain when $\mathbf{J}_T$ can be related to the electric field by a generalized Ohm's law,

$$\mathbf{J}_T = (\sigma + i\omega\varepsilon)\mathbf{E}, \quad (17)$$

where the complex quantity in brackets is known as the admittivity of the medium.

In EM prospecting at low frequencies, any magnetic field generated by the displacement current term $\partial \mathbf{D}/\partial t$ is usually (although not always) negligible. Removal of $\partial \mathbf{D}/\partial t$ from equation (15) eliminates the wave nature of the EM field in free space so no propagation delay will be predicted. This result is usually called the quasi-static approximation (or the EM field is said to be quasi-stationary). According to the quasi-static approximation, the primary magnetic field in free space generated by a local source loop of alternating current I is everywhere in-phase with I; and the primary electric field is everywhere in quadrature with I, being generated by the time derivative of the magnetic field.

MAGNETIC FIELD OF CURRENTS

In many EM prospecting problems, we can consider the EM field to be generated entirely from two electric current distributions; one being an externally supported current in a transmitter wire or coil $\mathbf{J}'$, the other being $\mathbf{J}_c$ the density of conduction current impressed into the earth according to Ohm's law. The magnetic field of these currents is derived from

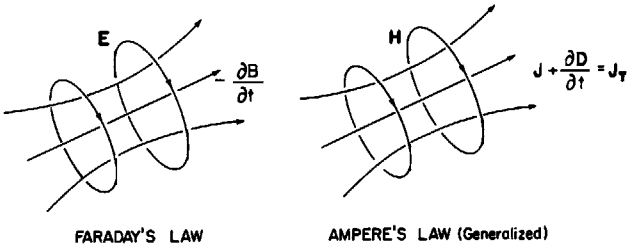

Fig. 2. The circulation relationships between the electric and magnetic fields according to Faraday's and Ampere's laws.

$$\nabla \times \mathbf{H} = \mathbf{J} = \mathbf{J}_c + \mathbf{J}' \tag{18}$$

which has a general solution known as the Biot-Savart equation.

$$\mathbf{H}(\mathbf{r}) = \frac{1}{4\pi}\int_v \frac{[\mathbf{J}_c(\mathbf{r}_0) + \mathbf{J}'(\mathbf{r}_0)] \times (\mathbf{r} - \mathbf{r}_0)}{|\mathbf{r} - \mathbf{r}_0|^3}\, d^3\mathbf{r}_0 \tag{19}$$

(Note that $\mathbf{J}_c$ and $\mathbf{J}'$ must together form a continuous, divergence-free circulation for this equation to calculate a physically realizable field).

A routine application of equation (18) is in calculating the free-space primary magnetic field of a known source current. Two specific cases are frequently needed, a small loop of radius a carrying current I which approximates a magnetic dipole and a straight current wire which is long compared to the distance at which its magnetic field is observed. These cases are illustrated in Figure 3. For the case $a \ll \sqrt{\rho^2+z^2}$ where the loop- can be considered small, and defining the moment of the loop as $m = \pi a^2 I$, we have

$$\mathbf{H}_\rho = \frac{m}{4\pi}\frac{3\rho z}{(\rho^2 + z^2)^{5/2}}$$

$$\mathbf{H}_z = \frac{m}{4\pi}\frac{(2z^2 - \rho^2)}{(\rho^2 + z^2)^{5/2}}\,. \tag{20}$$

In spherical coordinates we can write equation (20) as

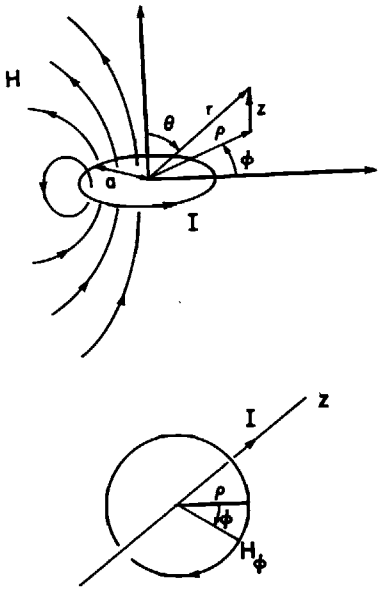

Fig. 3. Magnetic field about a current loop and a current line.

$$\mathbf{H}_r = \frac{m}{4\pi}\frac{2\cos\theta}{r^3}$$

$$\mathbf{H}_\theta = \frac{m}{4\pi}\frac{\sin\theta}{r^3} \tag{21}$$

so the magnetic field strength drops off as the inverse cube of distance from the source. For the long wire, the field is an azimuthal circulation

$$\mathbf{H}_\phi = \frac{I}{2\pi\rho} \tag{22}$$

and the fall-off is as inverse distance from the wire.

In modeling induction of eddy currents in the earth, the source current and the earth's physical property distributions are known. Although the induced current system is unknown there are two basic approaches to finding the system. One approach is to divide the EM field into two partial fields, a primary component defined as the field which the externally maintained sources would generate in some reference earth model (often free space), and a secondary component which is the remainder necessary to make up the correct total. The other approach is to consider only the total field. We shall use both approaches, but the primary-secondary separation often has heuristic and computational advantages because the relationship of the fields to the currents impressed in the earth is made clearer.

THE ELECTRIC FIELD

Before considering the external magnetic fields, we need to discuss the behavior of the electric fields and associated current systems within the ground. In particular, we need to understand the effects of electrical inhomogeneity. The important concepts of depolarization and current channeling number are introduced for later use.

At low frequency, an effective method for creating an electric field in a conductor is to connect a source of current to the conductor. A positive source current connected to a point in the interior of a uniform conductor injects positive charge at the contact, which in turn creates a radial electric field. The electric field creates a radial conduction current according to Ohm's law. When the source current is first switched on, charge will immediately collect at the contact point in an amount such that continuity will be achieved between the source and the conduction current. Note that the configuration and strength of the electric field in the uniform conductor depends on the location of the source current's terminations rather than on the path of the current in the insulated wire (Figure 4).

In an insulating region, a static source distribution of charge or charge dipoles (such as might be produced in a material which has strongly polar molecules) can create a continuing electric field. But in a conducting region, this field cannot be maintained without a continuing source of current because charge will immediately be transferred by the conduction currents in an amount sufficient to neutralize the static charge distribution and nullify its electric field. Thus, only source *current* distributions need be considered as sources of a static or very low frequency electric field in any but the most insulating of regions.

In practice, the source currents of EM exploration are usually lines of current in transmitter wires rather than continuous distributions of source current density $\mathbf{J}'$. Continuous distributions of source current usually arise only in computational modeling as a mathematical artifice analogous to dielectric polarization and to magnetization in order to represent the extra conduction current which flows in a "target body" whose conductivity σ_b is anomalous in comparison with its "host" surroundings (Figure 5). The density of conduction current in the anomalous region is considered to be partly a normal conduction current and partly a source current (usually denoted as $\mathbf{J}_a$ and called an anomalous current or scattering current), with both considered to be flowing in the host material.

$$\mathbf{J} = \mathbf{J}_c + \mathbf{J}_a = \sigma_h \mathbf{E} + \mathbf{J}_a,$$

where

$$\mathbf{J}_a = \sigma_a \mathbf{E}$$

and

$$\sigma_a = \sigma_b - \sigma_h. \tag{23}$$

In this approach, the anomalous body is considered not as a region of different conductivity, but instead as a region within the host region wherein there is an anomalous density of source current.

Spatial inhomogeneity of conductivity affects the EM field in two ways. First, the electric field will be directly distorted by the charge deposited at conductivity contrasts to ensure continuity of current flow (and if the frequency is sufficiently high, also at contrasts in dielectric polarizability). Second the electric field will be indirectly distorted by the induction of the electric field from the time-varying magnetic field of eddy currents. The former process is nearly instantaneous, i.e., essentially time invariant, whereas the latter is slow, i.e., rate-dependent. Overall, the induction process causes the total electric and magnetic fields to diffuse slowly into conductive regions. Both effects are important in EM exploration. They are discussed separately because the physics of the two cases differ.

The direct distortion of the electric field by spatial variations in the conductivity of the earth is easiest to study at very low frequency where any complications due to rate-dependent EM induction vanish. As mentioned, the effect of a conductivity inhomogeneity in an otherwise uniform host space is determined by finding the anomalous current distribution $\mathbf{J}_a$ within the target zone that will make the total current density everywhere divergence free. $\mathbf{J}_a$ is created by the total electric field according to equations (23) and the total electric field, in turn, creates a secondary electric field inside and outside the inhomogeneity.

In reality, the secondary electric field is generated by the concentration of charge which arises on the interface of the anomalous region when current flows through the field (where $\mathbf{J}_a$ is discontinuous and therefore $\nabla \cdot \mathbf{J}_a$ is non-zero). If the inhomogeneity is more conductive than the host medium, the charge creates a reverse secondary electric field inside the body which tends to cancel the primary field. If the homogeneity is

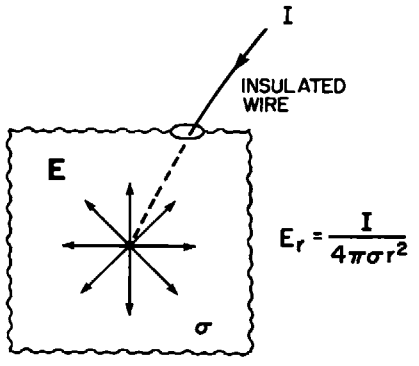

Fig. 4. Electric field created by injecting current into a conductive medium at the termination of an insulated source current line.

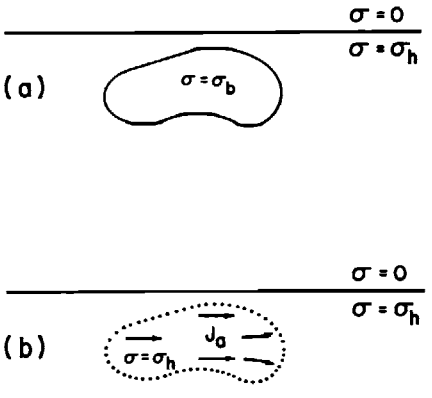

Fig. 5. A local zone of anomalous conductivity (a) can be treated as a zone of anomalous (source) current flowing in the host medium (b).

less conductive, the field inside the body is enhanced. The effect is called *depolarization* in exact analogy with the corresponding effect in a dielectric medium (and demagnetization in a magnetically permeable medium).

As an example, we analyze the case of a sphere in a uniform primary electric field. For this shape, both a uniform anomalous current density and a uniform secondary electric field are produced inside the sphere and a dipolar secondary field is produced outside. The strength of $\mathbf{J}_a$ depends on the conductivity contrast, i.e.,

$$E^s = -\mathbf{J}_a/3\sigma_h$$

and

$$\mathbf{J}_a = (\sigma_b - \sigma_h)\ (\mathbf{E}^p + \mathbf{E}^s)$$

giving

$$\mathbf{J}_a = \frac{3\sigma_h(\sigma_b - \sigma_h)}{\sigma_b + 2\sigma_h}\,\mathbf{E}^p. \tag{24}$$

Therefore the total amount of current flowing through the inhomogeneity is limited to something much less than $\sigma_b\mathbf{E}^p$, (i.e., to $3\sigma_h\mathbf{E}^p$) no matter how high σ_b becomes. The effect is opposite in the case of a resistive inhomogeneity, with the total current density then being forced to be larger than $\sigma_b\mathbf{E}^p$, i.e., ($3\sigma_h$ $\mathbf{E}^p/2$).

For modest conductivity contrasts, the strength of $\mathbf{J}_a$ is directly proportional to the primary electric field and to a measure of conductivity contrast which could be given the name "relative ohmic susceptibility" κ_σ in analogy with the magnetic and dielectric cases, i.e.,

$$\kappa_\sigma = \left(\frac{\sigma_b}{\sigma_h} - 1\right),$$

and

$$\mathbf{J}_a = \frac{\kappa_\sigma\sigma_h}{(1 + \kappa_\sigma/3)}\,\mathbf{E}^p \tag{25}$$

and thus

$$-1 < \kappa_\sigma < \infty.$$

However, the proportionality no longer holds at strong conductivity contrasts where depolarization causes $\mathbf{J}_a$ to saturate. The amount of depolarization is a strong function of the geometry of the anomalous body and the primary field, being minimal in a conductive inhomogeneity which is greatly elongated in the direction of the primary electric field, and extremely important if the along-the-field dimension is small in comparison to the across-the-field dimensions. The opposite is the case when the inhomogeneity is resistive, as can be seen by studying the depolarization of an ellipsoidal body. Just as for a sphere we can show that if the primary field is uniform and along a principal axis, the anomalous current density must also be uniform and create a uniform internal secondary electric field in the same direction. The proportionality between the anomalous current density and the internal field is written as $\mathbf{E}^S = -N\mathbf{J}_a\sigma_h$. The proportionality factor N (called the depolarization factor) takes a value between 0 and 1 depending, respectively, on whether the inhomogeneity is highly elongated or highly oblate in the direction of the current flow. The value is 1/3 for a sphere. The expressions for $\mathbf{J}_a$ and total $\mathbf{J}$ are then

$$\mathbf{J}_a = \frac{\kappa_\sigma\sigma_h}{(1 + N\kappa_\sigma)}\,\mathbf{E}^p \tag{26}$$

and

$$\mathbf{J} = \frac{\sigma_b}{(1 + N\kappa_\sigma)}\,\mathbf{E}^p. \tag{27}$$

The expression for $\mathbf{J}_a$ with κ_σ positive is graphed in Figure 6.

Although the depolarization phenomenon may become more complicated if the anomalous body is not ellipsoidal or if the primary field is nonuniform, the basic effect is universal. When a current flux crosses a conductivity interface, charge collects on the interface and adjusts to a level such that the secondary electric field generated is enough to keep the normal component of current density continuous. This effect can be represented as the creation of an anomalous current density inside the inhomogeneity whose strength will depend on the conductivity contrast. But, inside the anomalous region, the secondary electric field of the

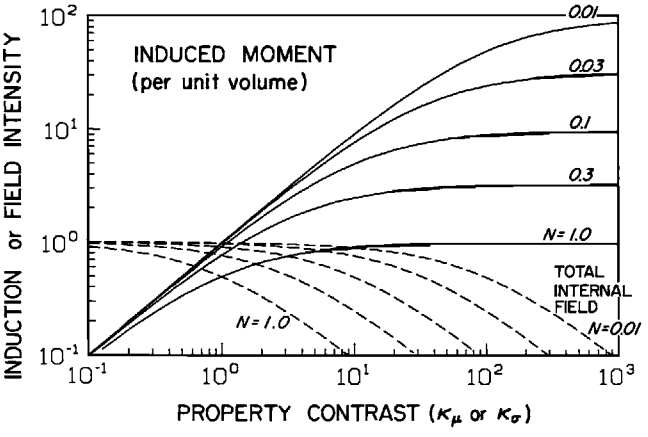

Fig. 6. The anomalous current or magnetization induced in an ellipsoidal conductivity inhomogeneity as a function of shape and conductivity contrast (from West and Edwards, 1985).

charge generally opposes the primary electric field if the body is conductive or will be enhanced if the body is resistive. If the conductivity contrast is made strong, this field will reduce the amount of anomalous current that can flow. In an ellipsoidal body, conductive saturation begins to take place when $\kappa_\sigma \approx 1/N$ and resistive saturation when $\kappa_\sigma \approx -(1 - N)$. In the former case, the anomalous current density limits at $(1/N)$ times the primary current density, in the latter at $-1/(1 - N)$ times. Similar dimensionless factors (analogous to the relative ohmic susceptibility normalized by depolarization factor) can be constructed for most geometries, and they are known as current channeling numbers. In further discussion of conductive inhomogeneities, we denote the current channeling number by α and assume that the number is normalized like $\kappa_\sigma N$ so that transition to saturation takes place at $\alpha \approx 1$. Thus, in any small conductive zone of volume V, the anomalous current $\mathbf{J}_a$ is approximately parallel to the primary electric field $\mathbf{E}^p$ and given approximately by

$$\mathbf{J}_a = \left(\frac{\alpha}{1+\alpha}\right)\left(\frac{\sigma_h \mathbf{E}^p}{N}\right). \tag{28}$$

The secondary electric field outside the body can be estimated roughly by considering the field to be produced by a source current dipole at the center of strength

$$\mathbf{j}_a = V\mathbf{J}_a = \left(\frac{\alpha}{1+\alpha}\right)\left(\frac{V\sigma_h \mathbf{E}^p}{N}\right). \tag{29}$$

Magnetic properties of the earth also affect the EM field. If the ground is magnetically permeable (i.e., has a nonvanishing magnetic susceptibility), spatial variations in permeability μ will have the same sort of time-invariant effect on the magnetic field as conductivity contrasts have on the electric field. However, permeability effects usually have only a minor influence on EM exploration. Except in a few highly magnetic formations, μ varies only slightly (<3%) in comparison to the several orders of magnitude of variation which is common in σ.

SKIN EFFECT

The simplest case of eddy current induction to solve mathematically is for an infinite uniform medium in which a laterally uniform field is created having only one vector component and a one-dimensional spatial dependence (z), i.e., the classical skin depth problem. Equations (15) are then easily simplified, combined, and solved for either **E** or **H** to give, in a uniform, sourceless region

$$\left(\nabla^2 - \sigma\mu\frac{\partial}{\partial t} - \varepsilon\mu\frac{\partial^2}{\partial t^2}\right)\begin{matrix}\mathbf{E}\\ \mathbf{H}\end{matrix} = 0 \tag{30}$$

or, if the time variation is a simple harmonic ($e^{i\omega t}$) then

$$(\nabla^2 + k^2)\begin{matrix}\mathbf{E}\\ \mathbf{H}\end{matrix} = 0 \quad k^2 = -i\omega\mu(\sigma + i\omega\varepsilon). \tag{31}$$

Equation (31) has one-dimensional solutions of the type

$$\mathrm{E}_x(z) = \mathrm{E}_{ox} \exp \pm ikz$$
$$\mathrm{H}_y(z) = \mathrm{H}_{oy} \exp \pm ikz$$

where the exponential has a negative sign for propagation in the positive z direction and

$$\frac{\mathrm{E}_{ox}}{\mathrm{H}_{oy}} = \frac{\omega\mu}{k}.$$

When $\sigma \gg \omega\varepsilon$, which is usual at audio frequencies and below, and if we consider the field to have its source in the $-z$ direction so that it propagates and attenuates in the $+z$ direction, we can write the quasi-static form of equation (31) as

$$\frac{\mathrm{E}_x(z)}{\mathrm{H}_y(z)} = \frac{\mathrm{E}_{ox}}{\mathrm{H}_{oy}} \exp(-z/\delta) \exp(-iz/\delta) \tag{32}$$

where

$$\delta \equiv \left(\frac{2}{\sigma\mu\omega}\right)^{1/2}, \quad \frac{\mathrm{E}_{ox}}{\mathrm{H}_{oy}} = -\left(\frac{\omega\mu}{\sigma}\right)^{1/2} e^{i\pi/4}, \tag{33}$$

i.e., the E and H fields are perpendicular to one another, and they both attenuate by a factor e and shift phase by 1 radian in a distance $\delta = \sqrt{(2/\sigma\mu\omega}$ which is called the skin depth. This is illustrated in Figure 7a. An interesting result known as the Cagniard relationship is obtained from the ratio of the electric and magnetic field components. The conductivity of the medium can be found from

$$\sigma = \mu\omega\left(\frac{H_y}{E_x}\right)^2. \tag{34}$$

The same results are easily found for the case of a uniform field steeply incident on the surface of an infinite conducting region (half space). An alternating EM field is prevented from penetrating into the conductor by formation of an induced current system near the surface. The (secondary) field of the induced current cancels the incident (primary) field inside the conductor.

The corresponding time domain expressions for a step-like magnetic field created at $t = 0$ are

$$\mathbf{H}_y(z) = \frac{1}{2} - \operatorname{erf}\left[\left(\frac{\sigma\mu}{2t}\right)^{1/2} \frac{z}{2^{1/2}}\right] \tag{35}$$

$$\mathbf{E}_x(z) = \frac{2^{1/2}}{\pi^{1/2}\sigma}\left(\frac{\sigma\mu}{2t}\right)^{1/2} \exp\left[-\left(\frac{\sigma\mu}{2t}\right)\frac{z^2}{2}\right]. \tag{36}$$

These expressions are the normal distribution and normal frequency functions of statistical theory with a variance $\sqrt{(2t/\sigma\mu)}$. The variance factor $\sqrt{(2t/\sigma\mu)}$ has units of length and is the time domain analog of skin depth, i.e., the factor is the distance the field diffuses in time t into a medium of conductivity σ. Figure 7b shows the spatial configuration of the fields at several successive instants. Penetration is proportional to the square root of delay time (time since the transient) or the inverse square root of frequency.

These results are very revealing, but they must not be assumed to apply quantitatively to fields which have a more complicated geometry, because the diffusion rate is also a function of field geometry. This function can easily be shown by including a harmonic spatial dependence $e^{-i(px + qy)}$ in the above equations, i.e., a spatial wavelength of $2\pi/p$ and $2\pi/q$ in the x and y directions. Writing $\lambda^2 = p^2 + q^2$, the z variation of the fields then becomes $\exp [i(\lambda^2 - k^2)^{1/2}]z$ which is to be compared with a variation of $e^{-\lambda z}$ when $|k|$ vanishes. The latter expression is just the (outward) continuation relationship for potential fields. Thus the additional multiplicative attenuation and phase shift factor due to conductivity of the medium is

$$\exp\{[\lambda - (\lambda^2 - k^2)^{1/2}]z\}$$

$$= \exp\left\{[\lambda\delta - (\lambda^2\delta^2 + 2i)^{1/2}]\frac{z}{\delta}\right\} \tag{37}$$

which for large spatial extent when $\delta \ll 1/\lambda$ becomes the usual skin effect attenuation

$$\exp -\left[(1 + i)\frac{z}{\delta}\right] \tag{38}$$

and for small spatial extent when $\delta \gg 1/\lambda$ becomes

$$\exp -(iz/\lambda\delta^2). \tag{39}$$

When the spatial scale of the field is much larger than the skin depth, attenuation takes place according to the plane wave skin depth formulas. But when the field is localized, (i.e., has mainly short wavelength components), it is progressively phase-shifted in passing to depth but is not attenuated in amplitude any more than would be the case if the field were static or in a free space.

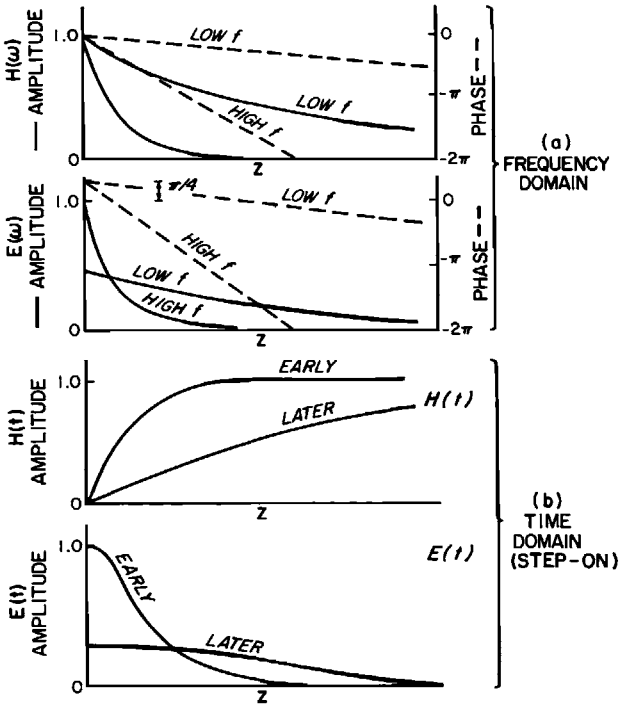

Fig. 7. Sketches showing the diffusion of laterally uniform electric and magnetic fields into a conductive medium: (a) The attenuation of an alternating magnetic field. (b) The diffusion of a step change in magnetic field.

EDDY CURRENTS IN AN IDEAL CIRCUIT

An elementary case which is discussed in every introductory explanation of EM prospecting is induction in a simple loop circuit—i.e., induction in a conductive loop of wire which is situated in free space and subjected to a time-variable magnetic field. Although this model does not permit quantitative modeling of induction in real, three-dimensional (3-D) conductors, the model does have great heuristic value and theoretical importance. The analysis is very simple because the current induced in a closed circuit has a known, fixed geometry (that of the circuit), whereas the current system induced in a 3-D conductivity distribution could have a wide variety of configurations. In a circuit, only the intensity of the induced current need be found.

If the circuit has a resistance R and inductance L, which gives a time constant $\tau = L/R$, and if the circuit is threaded by an alternating magnetic field from the source so that the primary flux is Φ^P, then the current I induced in the loop is (Grant and West, 1965)

$$I(\omega) = \left(\frac{-i\omega\tau}{1 + i\omega\tau}\right)\frac{\Phi^P}{L} = \left(\frac{-i\gamma}{1 + i\gamma}\right)\frac{\Phi^P}{L}. \tag{40}$$

If the frequency variable is taken as the dimensionless quantity $\gamma = \omega\tau$ (the inductive response parameter) and the current is measured as a fraction of the saturation level, all simple circuits respond identically. Figure 8 shows the frequency dependence of I in several different plotting forms that are common in EM exploration. The key point is that the induced current grows linearly with frequency until a saturation effect sets in. The response is a smooth transition between the so-called resistive (low frequency) and inductive (high frequency) limits of response. In the resistive limit, the resistance of the loop is large and the induced current which is in quadrature phase with the primary magnetic flux is so weak that the secondary magnetic flux which is produced in the loop is negligible. In the inductive limit, the secondary flux is so large that it becomes almost equal and opposite to the primary flux, giving a near vanishing total flux through the loop which, nevertheless, is sufficient to produce the eddy current.

The transition from resistive to inductive limit occurs over about a decade of frequency centered about $\omega = 1/\tau$. The time constant $\tau = L/R$ depends on the inductance and resistance of the circuit which in turn depend on its shape, size, and conductivity. For a conductive circuit of fixed shape having a scale size l, we can easily show that L/R is proportional to $\sigma\mu l^2$. The dimensionless response parameter γ is then seen to be proportional to $\sigma\mu\omega l^2$. Comparing this result with the skin depth relation from equation (33), we see that γ is thus also proportional to l^2/δ^2. The response parameter γ may be thought of as a dimensionless frequency or conductivity. Sometimes working with the dimensionless distance l/δ which is given the name induction number, is more convenient.

The spectral response of a loop circuit is a quotient of complex numbers in which the denominator has a root at $\omega = iR/L$ and the numerator has a root at $\omega = 0$. In the jargon of electrical engineering, the response is said to be characterized by a single pole and a zero, with the zero located at the origin of the complex frequency plane and the pole at R/L on the damping axis. The time-domain response of any finite linear network due to transient excitation is always made up of terms containing e^{-st}, where s is the complex frequency of each pole in the response. For a single loop with a single pole, there is only one such term which is a pure decay. We can easily show that the time-domain result of the induced current for a positive step in the primary magnetic flux $u(t)\Phi^p$ is

$$I(t) = \frac{\Phi^p}{L} u(t) e^{-t/\tau} \tag{41}$$

and for an impulse excitation, the result is

$$I(t) = \frac{\Phi^p}{L}\left[\delta(t) - \frac{1}{\tau} e^{-t/\tau}\right] \tag{42}$$

where $u(t)$ is the unit step function and $\delta(t)$ is the unit impulse. These results are illustrated in Figures 9 and 10.

To relate the above discussion to what is measured in practical EM exploration, we may consider an EM system consisting of a transmitter and a receiver loop. A conductor in the ground is represented by a third loop (Figure 11). The mutual inductances L_{ij} between each pair of loops can be calculated. They represent the magnetic flux cutting one loop (i) due to a unit current in another (j) and are symmetric in i, j. In a frequency domain EM system, the observed quantity might be the secondary voltage induced in the receiver measured in terms of the primary voltage, viz.,

$$e^s = -i\omega L_{23} I_2$$

and

$$e^p = -i\omega L_{13} I_1$$

where

$$I_2 = \frac{-i\omega L_{12} I_1}{R_{22} + i\omega L_{22}}$$

giving

$$e^s/e^p = -\left(\frac{L_{12}L_{23}}{L_{22}L_{13}}\right)\left(\frac{i\omega\tau}{1 + i\omega\tau}\right), \tag{43}$$

where

$$\tau = L_{22}/R_{22}.$$

The second factor in equation (43) is just the frequency response of the loop as previously discussed. The first factor is a real coefficient which expresses the geometrical coupling between the coils of the EM system (loops 1 and 3) and the target body (loop 2). This factor is the only part of equation (43) that will change if the EM system is traversed on a profile over the body, and the factor will determine the strength and profile form of the anomalous response. Understanding this factor is crucial to EM interpretation. The factor's significance is easier to visualize if we think of an inductance L_{ij} as the amount of magnetic flux that cuts circuit i due to a unit current in loop j. For loops in an insulating medium, this can be calculated using the Biot-Savart formula [equation (19)].

In summary, a study of frequency domain induction in a simple loop reveals that strength of the normalized response at saturation (inductive limit) depends only on loop geometry at the position of the EM system, whereas the time constant (L/R) involves both the

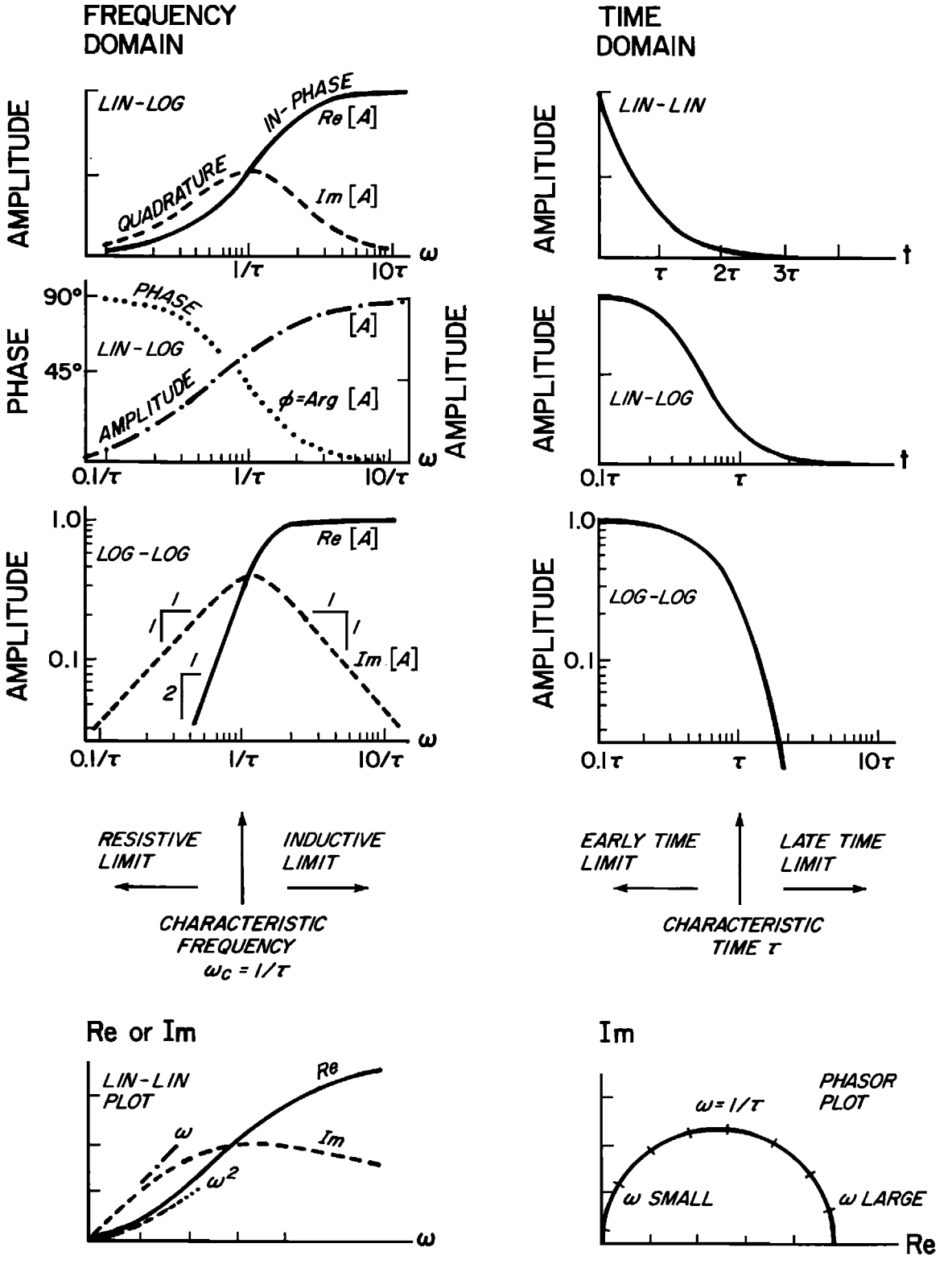

Fig. 8. Frequency response of the current induced in a simple loop circuit by an alternating magnetic field, shown in several plotting formats.

geometry and physical properties (conductivity). As a first order approximation, any eddy current system of restricted dimensions may be characterized by two parameters, its time constant and its strength at the inductive limit.

For a time domain system measuring voltage in a coil receiver and employing a sharp cut-off in transmitter current I as the source transient, the observed primary and secondary signals will be

$$e^p/I = L_{13}\delta(t)$$

$$e^s/I = \left(\frac{L_{12}L_{23}}{L_{22}}\right)\left(\frac{u(t)}{\tau}\right)\exp(-t/\tau) \qquad (44)$$

where $\delta(t)$ and $u(t)$ are, respectively, the Dirac delta and Heaviside step function.

The terms in these equations do not separate quite as neatly as in the frequency domain case. All have dimensions, so scale is important. In order to estimate the geometrical term from voltage measurements and thus to interpret something of the geometry of the target conductor, we must first determine the time constant of the response.

Because the induced current system flows in a closed loop, the system has a magnetic moment. To think of the induction process as creating a magnetic moment in the conductive body which tends to oppose the primary field and which thus partially deflects the total field away from the conductor often is helpful. In many respects, the process is analogous to what happens when a relatively insulating body in a more conductive host medium is subjected to a current field: An anomalous current density is created opposing the primary field whose intensity saturates as conductivity contrast is increased at a value where the primary current density is almost cancelled. However, there is a fundamental difference in phase characteristics because eddy current induction is dependent on the *rate of change* of primary magnetic field whereas charge induction is dependent on the primary electric field.

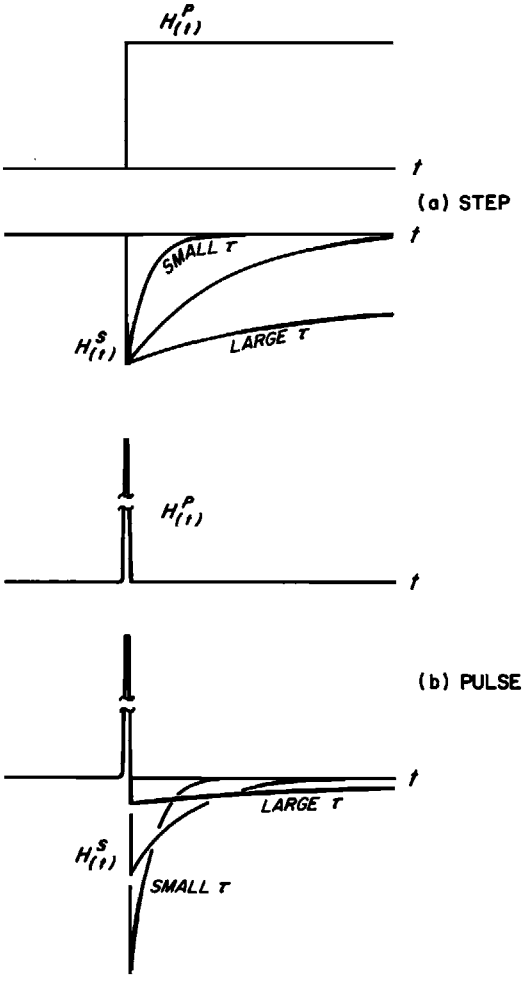

Fig. 9. Transient current induced in a simple circuit by (a) a step or (b) an impulse in primary magnetic field.

EDDY CURRENTS IN REAL CONDUCTORS

To find the eddy current pattern induced in a three-dimensional conductor of finite-size in an insulating host environment is more complicated than to find the

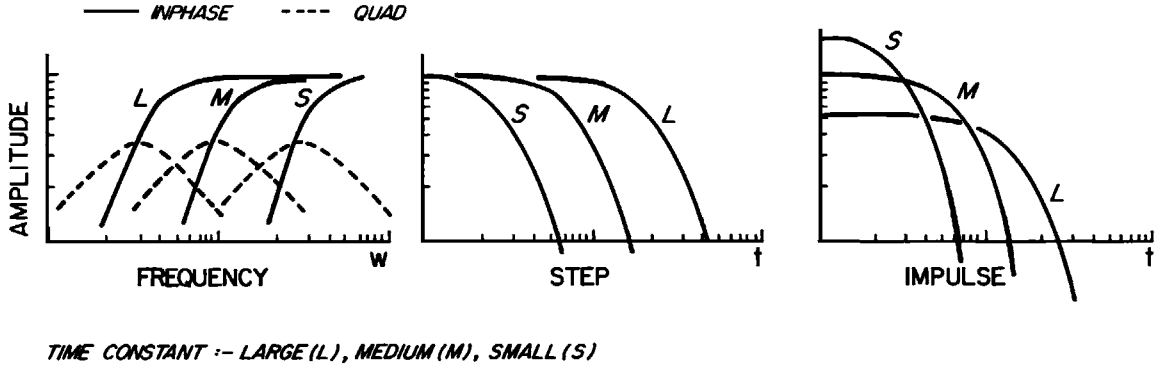

Fig. 10. Frequency and transient response of a simple circuit, showing the effect of changes in time constant.

pattern in an ideal loop circuit, but the physics does not differ essentially. The time-varying magnetic field causes a vortex of electric field to be induced in the conductive region subject to the condition that the field has no component normal to the boundary. Any possible normal component is immediately canceled by the depolarizing field of the surface charge which arises on the boundary because of the infinite conductivity contrast with the insulating surroundings. Then, any remaining electric field must be a divergence-free vortex generated entirely through Faraday's law.

The main complication to finding the configuration of the induced current system is that the pattern is not fixed. In general, the pattern will change if we alter the geometry or frequency of the primary field or the distribution of conductivity in the body. The effect of these complications on the conductor's spectral response is usually to spread the transition from resistive to inductive limits over a wide range of frequency (response parameter). A comparison between the frequency domain response of a conductive sphere in a uniform field and that of a circuit is shown in Figure 12. Both are plotted as functions of a dimensionless response paraemter ($\sigma\mu\omega a^2$ in the case of the sphere and $\omega L/R$ in the case of the circuit). The dimensionless response function is identical for all circuits but differs for bodies of different shape and conductivity distribution and, as will be discussed in a later section, the function also depends on the configuration of the primary field and the position where the secondary field is sensed. Some of the difference may correspond just to different scaling of the response parameter (i.e., to a lateral shift of the response curve when the curve is plotted with a logarithmic scale of response parameter). But there will also be, in general, some difference in functional form. Typically, the response of a 3-D conductor corresponds to the sum of several loop responses having a range of time constants. This response can be seen in Figure 12 where the slower variation is evident at large response parameters when compared to the single time-constant response of a simple circuit.

Not only does overall geometry of the conductor affect the spectral form of the response, but structure of the conductor at fine scale can also have an effect. If a laboratory experiment is done with a loop made of a single turn of copper wire, the observed spectral response near the inductive limit will not likely be well represented by equation (40). This lack of representation is because the inductance and the resistance of any real wire loop depends to some extent on the local distribution of current in the wire, whereas generally in theoretical calculations of inductance and resistance we assume that the current distribution is uniform over the wire's cross-section (such as does occur at low frequency). In designing electrical components, we usually account for the tendency of current to locate itself in the outer parts of the wire as frequency is raised (i.e., skin effect) by assigning a frequency-dependent complex resistance to the wire instead of trying to solve the three-dimensional EM modeling problem of a wire of finite thickness bent in some specific way. The engineering approach is useful because it permits us to allow in a simple way for fine structure in the current system. For instance, in a real experiment with a single turn wire loop, there will be a difference at high frequency if the wire is solid or if finely stranded, but the two cases are qualitatively similar and can be modeled in the same way using slightly different parameter values.

The ac resistance per unit length $R(\omega)$ of a long, straight uniform wire of radius a can be calculated quite easily (Smythe, 1968) and has a real component

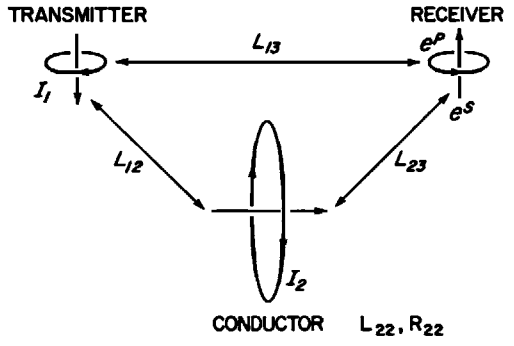

Fig. 11. Coupling of a simple circuit to the transmitter and receiver of a loop-loop EM system.

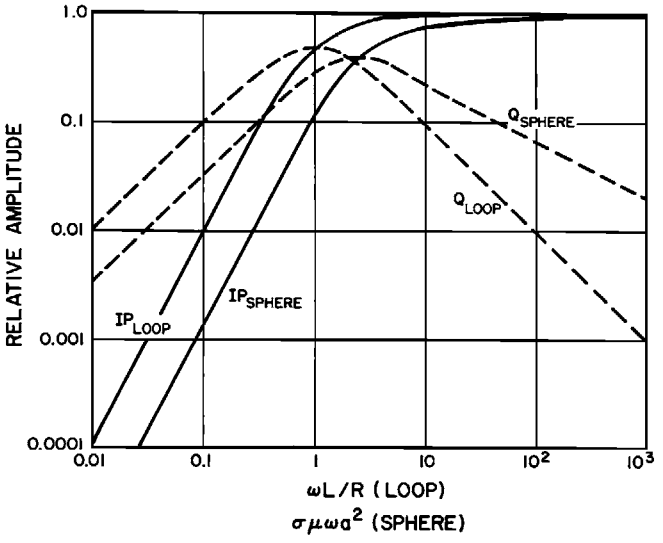

Fig. 12. Comparison between the frequency responses of a simple circuit and a spherical conductor in a uniform field.

$$R = \pi a^2 \sigma \left(1 + \frac{1}{12}\frac{a}{\delta} + \cdots\right) \quad a \ll \delta$$

$$\cong \pi a^2 \sigma \frac{1}{2}\frac{a}{\delta} \quad a > \delta. \tag{45}$$

Since the skin depth δ varies inversely as square root frequency, we see that the effective resistance rises as the square root of frequency, once skin effect becomes significant. Also, a part of the self inductance (the part known as the internal term and due to the magnetic field inside the wire) falls as $1/\delta$, so that the total impedance of the wire (not including the part due to external inductance) rises as $(2i\omega)^{1/2}$ at high frequencies. The total effect is that the inductive saturation effect seen in a simple circuit is significantly modified. The induced currents do not reach the inductive limit as quickly as the simple loop formula with constant (and real) L and R would suggest, and in extreme cases where the external inductance of the induced current system is so low that the internal term dominates (such as can arise in one and two-dimensional modeling problems), the induced current may have an approximate 45 degree phase angle with respect to the primary field over a broad range of conditions. In engineering jargon, this is equivalent to saying that the response can be represented as an infinite sum of single pole and zero responses wherein there is a continuous distribution of poles lying along the complex frequency axis over a very wide range of time constants.

The effects of fine structure are not trivial. Many geologic formations (especially those in which conduction is by electrolyic fluid in pores) may conduct in a relatively uniform manner, but base metal sulphide deposits often have a coarse network structure in which there are different degrees of interconnection at different scales. Induction in such bodies may exhibit a frequency response that differs distinctly from that of a uniformly conductive formation.

Spectral response is an important characteristic of a conductor; but equally important (if not more so) are the strength and geometry of the response. This strength and geometry must be predicted in order to interpret the position, shape, and size of a conductive feature from its EM response. Unfortunately, to solve completely for the eddy currents induced in a conductor of arbitrary shape at all frequencies is often difficult, but we can find the response at the inductive limit more easily.

At the inductive limit, the eddy currents create a secondary magnetic field which exactly cancels the primary field everywhere in the body. Since the eddy currents form a closed vortex, they can be represented as a distribution of magnetization which we denote as **U** to distinguish it from a true magnetization **M**, and then we can find the volume distribution of **U** which will nullify the primary magnetic field. This is a classic problem in static magnetism that can easily be solved numerically if an analytical method is not available. However, there is one crucial difference. Because $-dB/dt$ creates the electric field and the eddy currents, then the **B** field rather than the **H** field must be annulled. To see how this works, we may recall the depolarizing properties of a sphere as previously discussed.

In a sphere or along a principal axis of an ellipsoid, a uniform field is created by a uniform magnetization according to

$$\mathbf{H} = -N\mathbf{M}$$

and

$$\mathbf{B} = \mu_0(\mathbf{H} + \mathbf{M})$$

where $N = 1/3$ for a sphere. Thus for **U** to annihilate a primary field $\mathbf{B}^p$ at the inductive limit, it must take the value

$$\mathbf{U}_L = -\mathbf{B}^p/[\mu_0(1 - N)] = -\mathbf{H}^p/(1 - N)$$

giving a sphere a total induced moment m_L at the inductive limit

$$\mathrm{m}_L = (4\pi/3)a^3\mathbf{U}_L = -2\pi a^3\mathbf{H}^p \tag{46}$$

which is exactly what is predicted by the full solution.

The foregoing discussion leads to a convenient rough representation of eddy current induction in any body when the body is small enough that the primary field over the body is reasonably uniform. Approximating the spectral characteristics as a pole and zero response, we may write (for one principal axis)

$$m = -\left[\frac{i\gamma}{1 + i\gamma}\right]\left[\frac{VH^p}{1 - N}\right] \tag{47}$$

where m and H^p are components of the moment and field along the principal axis, $\gamma \approx \sigma_b \mu \omega abc$ and a, b are appropriate dimensions of the body akin to radius in the sphere case. Equation (47) is interesting when compared to equation (29), in which the anomalous current dipole produced in a conductive inhomogeneity by the electric field is given.

To calculate the response of a conductor to an EM system, we must work out the primary field at the body due to the transmitter and the secondary field at the receiver due to the moment induced in the body. To the extent that the target body can be considered reasonably small in comparison with the distances from the body to the transmitter and receiver (and assuming as is common that the coils of the EM system are negligibly small also), it is possible to consider only the values for one representative point

in the conductor. Then, we need only to make point-to-point calculations using dipole formulas.

The field of a dipole source is a (second rank) tensor quantity, since the source and the field are both vectors and in general each have three components. We could write

$$H_j = G_{jk}^{Hm} m_k \tag{48}$$

where the j and k subscripts stand for one of three orthogonal coordinate directions and the Hm superscript indicates that G is the function that relates magnetic field to magnetic dipole moment. However, to keep the discussions simple, we shall assume that we know the direction of induction in the conductor and the orientation of the coils of the EM system, so we require only the field in a given direction from a dipole of known orientation. Then we can symbolize the body-to-receiver and transmitter-to-body couplings as

$$H_r^s = G_{rb}^{Hm} m_b,$$

$$H_b^p = G_{bt}^{Hm} m_t$$

where G is now a scalar function and the subscripts now refer to the position of the field point and the dipole source. The directions of the components are assumed to be known. This knowledge immediately allows us to write an expression for the approximate normalized response of an EM system to a small target body as

$$e^s/e^p = H_r^s/H_p^s = \left[\frac{G_{rb}^{Hm}\, G_{bt}^{Hm}}{G_{rt}^{Hm}}\right] \times \left[\frac{V}{1-N}\right]\left[\frac{i\gamma}{1+i\gamma}\right]. \tag{49}$$

This expression is very similar to the result for the circuit model except that all the terms in equation (49) can now be estimated numerically.

Later we shall use the G notation to represent dipole field calculations of other kinds, so we introduce them all here. There are four possible types.

$$H = G^{Hm}{}_m, \quad E = \frac{1}{\sigma_h} G^{Ej} j,$$

$$E = i\omega\mu G^{Em}{}_m, \quad H = G^{Hj} j. \tag{50}$$

In these expressions, we have arranged that the quantity denoted by G is always real and constant at very low frequency and has dimensions of [length]$^{-3}$ (upper line) or [length]$^{-2}$ (lower line) irrespective of what sort of medium we assume the fields propagate through. However, we shall need only to make calculations for quasi-static fields in free space or relatively insulating media, and then the G functions are independent of frequency or conductivity.

DIPOLE SOURCE IN A CONDUCTIVE MEDIUM

The most commonly used source for EM prospecting is a small current carrying loop, which is essentially a magnetic dipole of moment $m = \pi a^2 nI$ (a radius, n number of turns, I current). In the quasi-static approximation, the magnetic field produced by a magnetic dipole in free space has the same time variation as the dipole, and its strength falls off inversely as the cube of distance in expression (20). The field of an alternating magnetic dipole in an infinite uniformly conductive medium is more complicated. The expressions for that field are derived in most EM theory texts and are given below. A sketch of the field configuration near the source is shown in Figure 13 for

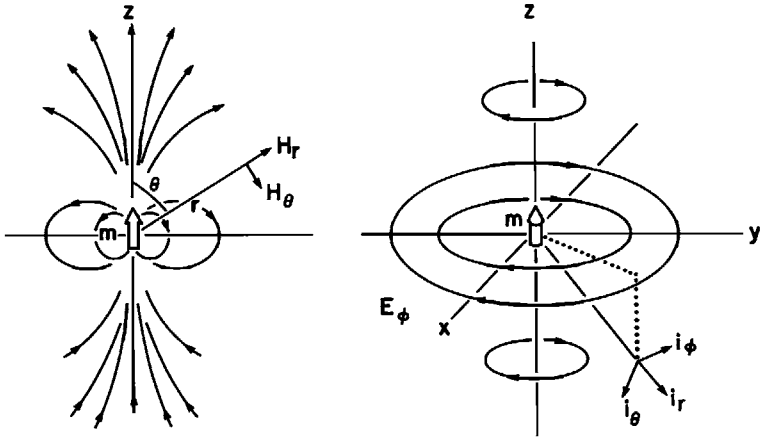

Fig. 13. Geometry of the EM field of an alternating magnetic dipole in an infinite uniform space. The direction of Eϕ reflects the negative sign of equation (53).

an axially directed magnetic dipole at the origin of a spherical coordinate system and in Figure 14 for a similar current dipole. Displacement currents have not been neglected, but the equations are given in two forms—one for an insulating (dielectric) and one for a conductive medium. The results are most simply described in terms of a dimensionless frequency or conductivity $\beta = |k|r^2$ (response parameter) or a dimensionless distance $|k|^{1/2}r$ (induction number), where $k^2 = -i\omega\mu(\sigma + i\omega\varepsilon)$. The three zones are defined as; near, intermediate, and far in which $r \ll, \approx, \gg |k|^{-1/2}$, respectively. In the insulating dielectric case where the dominant physics is wave propagation, the scale distance $|k|^{-1/2}$ is the radian wavelength $\Lambda/2\pi$. In the conductive case where diffusion dominates, the radian wavelength is nearly the skin depth of the medium, i.e., $\delta/\sqrt{2}$.

$$H_r = \frac{m}{4\pi}\frac{2\cos\theta}{r^3}(1 + ikr)\exp - ikr$$

$$= \frac{m}{4\pi}\frac{2\cos\theta}{r^3}\left[1 + \frac{(1+i)r}{\delta}\right]\exp - (1+i)r/\delta$$

$$= \frac{m}{4\pi}\frac{2\cos\theta}{r^2}\left[1 - \frac{ir^2}{\delta^2} + \frac{2(1-i)r^3}{3\delta^3} + \frac{r^4}{2\delta^4}\cdots\right] \quad (51)$$

$$H_\theta = \frac{m}{4\pi}\frac{\sin\theta}{r^3}[1 + ikr - k^2r^2]\exp - ikr$$

$$= \frac{m}{4\pi}\frac{\sin\theta}{r^3}\left[1 + \frac{(1+i)r}{\delta} + \frac{2ir^2}{\delta^2}\right]$$

$$\times \exp - (1+i)r/\delta \quad (52)$$

$$E_\phi = -\frac{m}{4\pi}\frac{\sin\theta}{r^2}(i\omega\mu)(1 + ikr)\exp - ikr$$

$$= -\frac{m}{4\pi}\frac{\sin\theta}{r^2}(i\omega\mu)\left[1 + \frac{(1+i)r}{\delta}\right]$$

$$\times \exp - (1+i)r/\delta \quad (53)$$

$$E_r = \frac{j}{4\pi\eta}\frac{2\cos\theta}{r^3}[1 + ikr]\exp - ikr$$

$$= \frac{j}{4\pi\eta}\frac{2\cos\theta}{r^3}\left[1 + \frac{(1+i)r}{\delta}\right]\exp - (1+i)r/\delta$$

$$= \frac{j}{4\pi\eta}\frac{2\cos\theta}{r^3}$$

$$\times \left[1 - \frac{ir^2}{\delta^2} - \frac{2(1-i)r^2}{3\delta^3} + \frac{1}{2}\frac{r^4}{\delta^4}\cdots\right] \quad (54)$$

$$E_\theta = \frac{j}{4\pi\eta}\frac{\sin\theta}{r^3}[1 + ikr - k^2r^2]\exp - ikr$$

$$= \frac{j}{4\pi\eta}\frac{\sin\theta}{r^3}\left[1 + \frac{(1+i)r}{\delta} + \frac{2ir^2}{\delta^2}\right]$$

$$\times \exp - (1+i)r/\delta \quad (55)$$

$$H_\phi = \frac{j}{4\pi\eta}\left(\frac{\theta\sin\theta}{r^2}\right)\eta\,[1 + ikr]\exp - ikr$$

$$= \frac{j}{4\pi\eta}\left(\frac{\theta\sin\theta}{r^2}\right)\eta\left[1 + \frac{(1+i)r}{\delta} + i\frac{r^2}{\delta^2}\right]$$

$$\times \exp - (1+i)r/\delta \quad (56)$$

where η is the admittivity $(\sigma + i\omega\varepsilon)$.

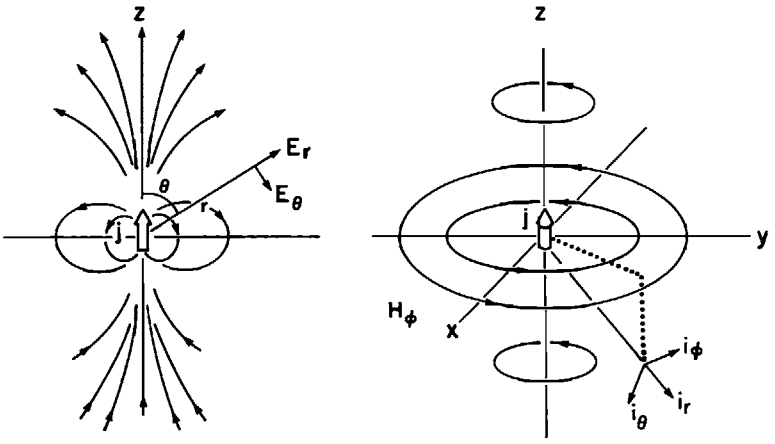

Fig. 14. Geometry of the EM field of an alternating electric current dipole in an infinite uniform space.

The points to note from the preceding are the following:

(1) In the near zone of an alternating magnetic dipole, the magnetic field is everywhere in-phase with the dipole current and its form and amplitude are the same as a static dipole. The electric field circulates around the dipole axis and is in quadrature phase with the dipole current and proportional in amplitude to ω.

(2) The transition from near to intermediate zone takes place when the quadrature component of secondary magnetic field due to eddy currents begins to be noticeable, increasing as $(r/\delta)^2$. Further out, the quadrature component is modified and a negative in-phase secondary magnetic field begins to appear as $(r/\delta)^3$; i.e., we can think of the current induced in the earth as being negligible (in a fractional sense) out to a certain range of r. Beyond this, a quadrature current is encountered first, and at even larger radius some in-phase induced current is found.

(3) At large distances, the field has a completely different r dependence than near the source. In the dielectric case, the fall-off of amplitude eventually moderates as the radiation field in which amplitude varies as $1/r$ becomes dominant. In the conductive case, the field begins to attenuate rapidly in an exponential manner, becoming vanishingly small beyond a few skin depths.

The equations for the electric current dipole have almost the same form as those of the magnetic dipole except the roles of **E** and **H** are interchanged. An electric dipole is a short linear current element which at its ends injects and removes conduction and/or displacement current from the surrounding medium. At the static limit (i.e., in the near zone) in a conductive medium, we have just the usual dc resistivity and magnetometric resistivity formulas for the fields of a buried source current. The given equations do not change if the current element is in a dielectric or conductive space. There certainly is a considerable practical difference between operating a current source in a conductor or in a dielectric, but the difference lies in the electric potential difference required from the energy source to cause the specified current to flow. In a conductive space, a source of constant voltage will produce about the same current at any frequency, whereas a similar source in a dielectric space will only inject appreciable current (i.e., displacement current) at very high frequency. In practice, to be able to inject displacement currents into an insulator, the current element must be made a resonant length in order to lower its impedance.

In some EM exploration methods, the source has appreciable size. An extended source can be treated numerically, simply by considering the source to be a line or surface distribution of dipoles. A large loop source can be represented as a surface distribution of magnetic dipoles or as a closed lineal distribution of current line elements. However, the latter approach is the only one available if the source current is grounded rather than closed. Treating a closed loop as a sum of current dipoles is straightforward for calculating the magnetic field, but may be confusing or inaccurate for electric field calculations. Most of the electric field of a current dipole at low or moderate frequency is due to the current divergence at the ends of the dipole. If the current line closes on itself, all the divergence-caused parts will cancel. The remainder should be the small time- or frequency-dependent induced electric field but it may possibly become lost in the round-off error of numerical calculations.

SOURCES ON A HALF SPACE

The formal analytical solutions for the EM fields of a source on a uniform half-space or a layered earth in which the conductivity $\sigma(z)$ varies only in one dimension have been in the literature for the best part of a century (Ward and Hohmann, 1988, Volume 1). However, they involve integrals of oscillating Bessel functions which often must be integrated numerically. Only in the past two decades has it been relatively easy to calculate results for such cases. Even now, computations of response at high frequency where no quasi-static approximation can be made are laborious. Time domain solutions are also still laborious to obtain (Goldman and Fitterman, 1987), although results can be synthesized from frequency domain solutions by Fourier transformation or from s domain solutions using the Gaver-Stehfest algorithm. Although much of the physics of the half-space problem is common with the whole-space problem discussed previously, there are also important differences. They arise because part of the field is in free space where it suffers no ohmic attenuation, in sharp contrast to the part which diffuses through the conductive medium.

Figures 15 and 16 show quasi-static results for an alternating vertical magnetic dipole (horizontal loop) on the surface of a uniform half space. Figure 15 shows amplitude response for a variety of geometries as a function of response parameter $\beta = \sigma\mu\omega r^2$. Figure 16 shows phase and amplitude of the field components generated by a vertical magnetic dipole. From Figure 15 we see that the total magnetic field near the source ($\beta < 1$) differs little from the free space field of the dipole. Focusing on the response of a vertical dipole (Figure 15, cases I and IV, and Figure 16) and considering how the field varies in comparison to free space values as the observation point moves outward on the surface along a radius, we see that the vertical component of the field begins to change amplitude and

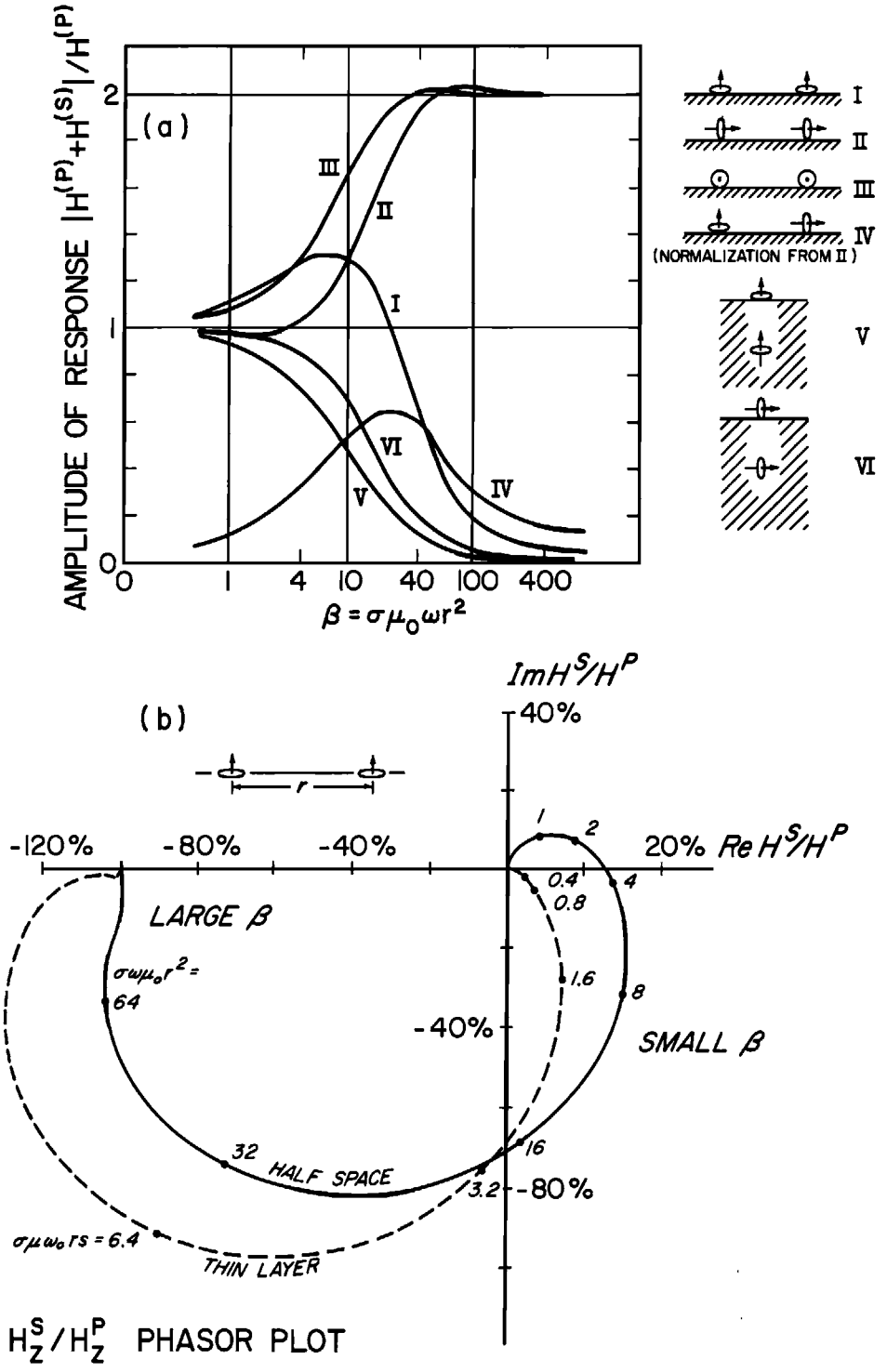

Fig. 15. (a) Normalized amplitude of the magnetic field generated by an alternating vertical magnetic dipole on the surface of a conductive half space (after Wait, 1951b). (b) Phasor plot of case I, with the response of a thin conductive layer shown for comparison (Eadie, 1979).

phase as $\beta \gg 1$ and eventually is reduced to near zero, i.e., the secondary vertical field eventually becomes nearly equal and opposite to the primary field.

A surface vertical dipole source generates no primary (i.e., free space) horizontal component of magnetic field at the surface, so this component must arise solely from currents induced in the ground. The component is a rough measure of the relative strength and phase of the induced current vortex flowing underneath the observation point. Moving outward from the source, the horizontal component (normalized to the primary vertical magnetic field, case IV) first becomes evident in the quadrature phase, becomes stronger and shifts through in-phase, and then dies away at large distance as the phase moves to −45°. If the total magnetic field is observed as an ellipse of polarization, the field will be linearly polarized and vertical near the source, and then will become elliptically polarized at larger distance. At even larger distance, the ellipse tilts and its principal axis becomes horizontal.

At large distance, the amplitudes of both the vertical and horizontal magnetic field fall off much more rapidly than they would in free space. In the rapid fall-off region ($r > 3\delta$), the electric and horizontal magnetic fields on the surface begin to obey the Cagniard equation [equation (34)]. Rapid attenuation in the far field can be understood by realizing that the current cirulation induced in the earth forms essentially a diffuse, oppositely directed image of the source within about a skin depth of the source loop. The field of this circulation cancels most of the primary field, with the cancelation becoming more complete as the observation point is taken to large radius.

In the near source zone where the secondary magnetic fields are weak, the electric field of an alternating magnetic dipole approximates the whole space equation [e.g., equation (53)]. E and therefore J fall off from the source as r^{-2}. Thus they rise steadily in comparison to the primary magnetic field which falls off as r^{-3}. Figure 17 shows how the electric field varies from the near to far zone.

There are several important differences in the EM field when an alternating magnetic dipole source is oriented with its axis along the surface of the half space. In the near-zone, the magnetic field is just what would be found in free space. However, the near-zone electric field is entirely different from the free space or uniform medium case. In a uniform medium, the electric field of a horizontal dipole would circulate about the horizontal dipole axis, with the field lines at the surface perpendicular to the earth-air interface. But because air is so highly insulating in comparison to almost all in-situ earth materials, the conductivity

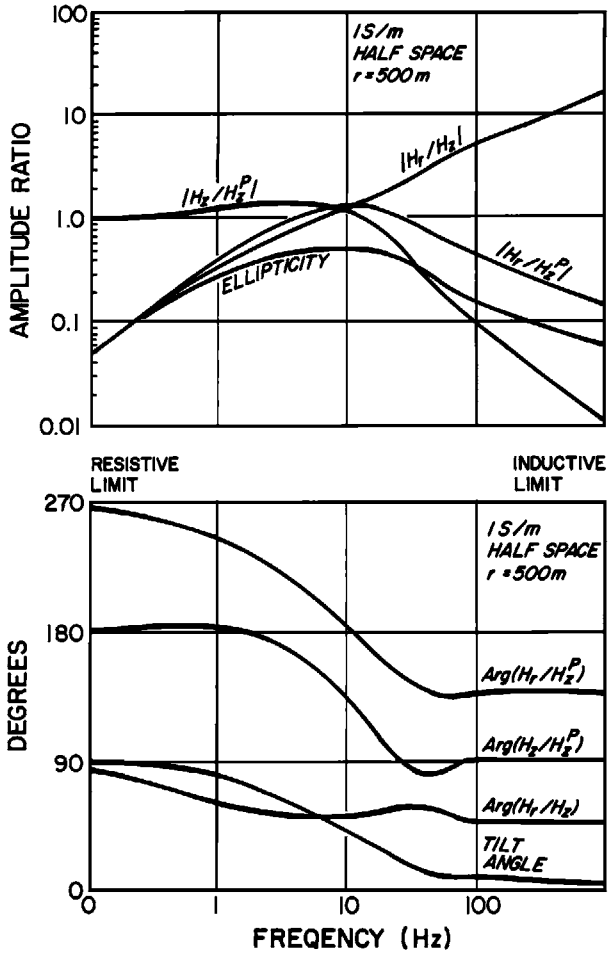

Fig. 16. Phase and amplitude of the vertical and horizontal magnetic field components and parameters of the polarization ellipse as a function of distance from an alternating vertical magnetic dipole source on an conductive half space.

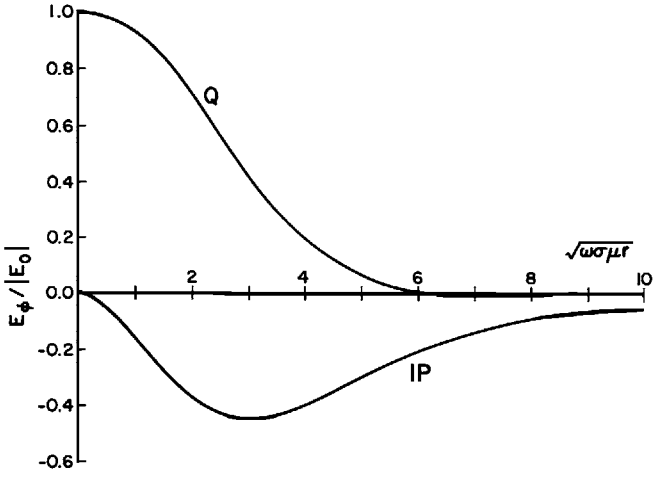

Fig. 17. Normalized in-phase and quadrature components of the electric field about an alternating vertical magnetic dipole on conductive half space (courtesy of B. Polzer).

contrast at the earth's surface is virtually infinite; and even if displacement currents are taken into consideration, the admittivity contrast is huge for any EM prospecting frequency. Since the normal component of total current density (conduction + displacement) must be continuous through a boundary, a charge distribution and a corresponding jump in the normal component of **E** must occur there.

The secondary E field of the interface surface charge neutralizes most of the E field that would otherwise exist within the earth, and it increases the E field in the air. The only part of **E** which continues to be found in the earth is a circulation about the primary magnetic field lines which penetrate into the earth. The situation is sketched in Figure 18. A corollary of this reasoning is that an above-surface time varying magnetic source cannot produce an appreciable component of electric field or current in a stratified earth normal to the layering. The strong conductivity or admittivity contrast at the earth-air interface always nullifes any vertical component of the E field as it passes into the earth.

The secondary magnetic field of a horizontal alternating dipole on a half-space behaves qualitatively much like that of a vertical dipole. In the near zone, the secondary field is so weak that the total field is virtually unperturbed (in a fractional sense) from its primary (free-space) form. As the observation point moves outward, a significant secondary field is encountered which eventually becomes so large (relatively) that it doubles the horizontal field of the source (Figure 15, cases II, III). The currents induced in the earth behave approximately like a shallow image dipole source, but the image in this case is parallel with the primary dipole. At intermediate ranges, the image analogy is very inexact, and appreciable vertical magnetic field is produced by the induced current system (case VI).

The preceding discussion has been in terms of increasing distance of the observation point from the source. Since distance must be measured in units of the skin depth (δ) which changes with frequency, the same remarks can be applied to a fixed observation point but with an increasing frequency of excitation. A useful terminology describes the observation point for a particular excitation frequency as lying in either the *near zone* where the secondary field is relatively negligible, the intermediate zone or *active region* where the secondary field is comparable in strength to the primary field and where the main eddy currents lie more or less underneath the observation point, or the *far zone* where the secondary field is comparable to and may nearly annihilate or double the primary field, and where in comparison to r the total field penetrates relatively little (i.e., δ) into the ground. For the far region, all of the main eddy current vortex lies between the observation point and the source. In simple cases such as a conductive half space where there is only one scaling distance, the zones correspond to $r \ll \delta$, $r \approx \delta$, $r \gg \delta$. At even greater distances, it may be necessary to consider propagation effects in the air (i.e., displacement currents). In the so-called *wave zone*, where $r > \approx \Lambda$, wave propagation becomes the significant physics.

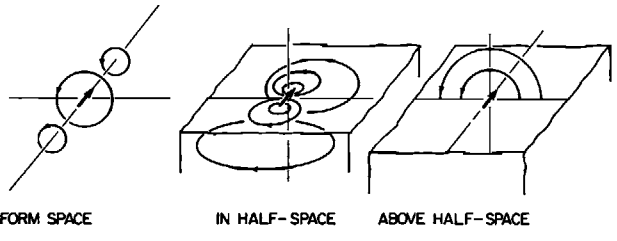

Fig. 18. Sketch of the effect of the air-earth interface on the electric field of a horizontal alternating magnetic dipole.

Many features of the responses shown in Figures 15 and 16 are also found in the response curve (Figure 8) for induction in a simple circuit. At a fixed distance, any secondary field component makes a transition with increasing frequency from a negligible amplitude to a saturation level (inductive limit). However, the quantitative form of the response may be substantially different from the single pole and zero response of a circuit. As an example, Figure 15b shows a phasor display of the vertical secondary field from a vertical dipole source on a half-space and an infinite thin sheet. The response near the low- and high-frequency limits is much more structured than the semicircular graph for a simple circuit. The complications arise mainly because the induced currents are spread throughout a large region and they move relative to the observation point as frequency or conductivity is changed. The inductive coupling between the current system and a field detector of given orientation may thus change strength and sign as the current moves. There is also potential for complicated interactions between various parts of the current system, particularly if the earth conductivity is strongly stratified.

Diffusion of an EM field from a point source into a conductive earth can also be studied in the time domain. Just as in the one-dimensional problem described in a previous section there are strong similarities between frequency domain and time domain cases. For very short times after a sharp discontinuity in the source current, all observation points will be in the far zone. As time progresses, the active range sweeps out to increasing distance and eventually leaves all the observation points in the near zone of response. There are, however, some important com-

plications. The closest parallel between frequency and time domain response is found when comparing the changing pattern of in-phase current with decreasing frequency with the changing pattern of induced current following a step transient in source current. But, commonly in transient EM systems the magnetic field is monitored using the voltage induced in a coil receiver so dB/dt is measured. Another difference arises from the conventional methods of viewing the data. In the examples given in frequency-domain, we plotted the fractional strength of the primary and secondary magnetic fields. However in time-domain, it is absolute rather than relative field strength which usually is recorded, since the primary field is usually not available for measurement during the observation period. Comparisons between frequency- and time-domain responses must take account of different normalization practice.

Nabighian (1979) has solved for the current system induced by a step change in the strength of a horizontal loop lying on a half-space and has aptly described the current system as an expanding and sinking smoke ring (Figure 19). For a step transient current in any kind of loop lying directly on a uniformly conductive ground, the induced current begins as an image of the source current flowing immediately under the source wire. Essentially, the total current in and near the source wire remains constant, so when the source current turns off, a similar ground current starts up. The current system in the ground then expands and diffuses at a time-varying rate which depends on ground conductivity. The diffusion distance increases with the square of the ratio of time to conductivity.

The description of the transient eddy current system as an expanding smoke ring is apt, no matter whether absolute or relative field strengths are considered. However, the picture will be altered if the excitation is not step-like. For instance, if the source current is a pulse (or equivalently if induction by a step source current is monitored by observing the rate of change of secondary magnetic field), the initial smoke ring will be seen to be followed immediately by a ring of opposite polarity. The two will diffuse out together and eventually will merge and annihilate each other.

Examples of transient fields on the surface of a conducting earth for the step response of a dipole transmitter are illustrated in Figure 20.

Grounded wires are not so widely used as sources

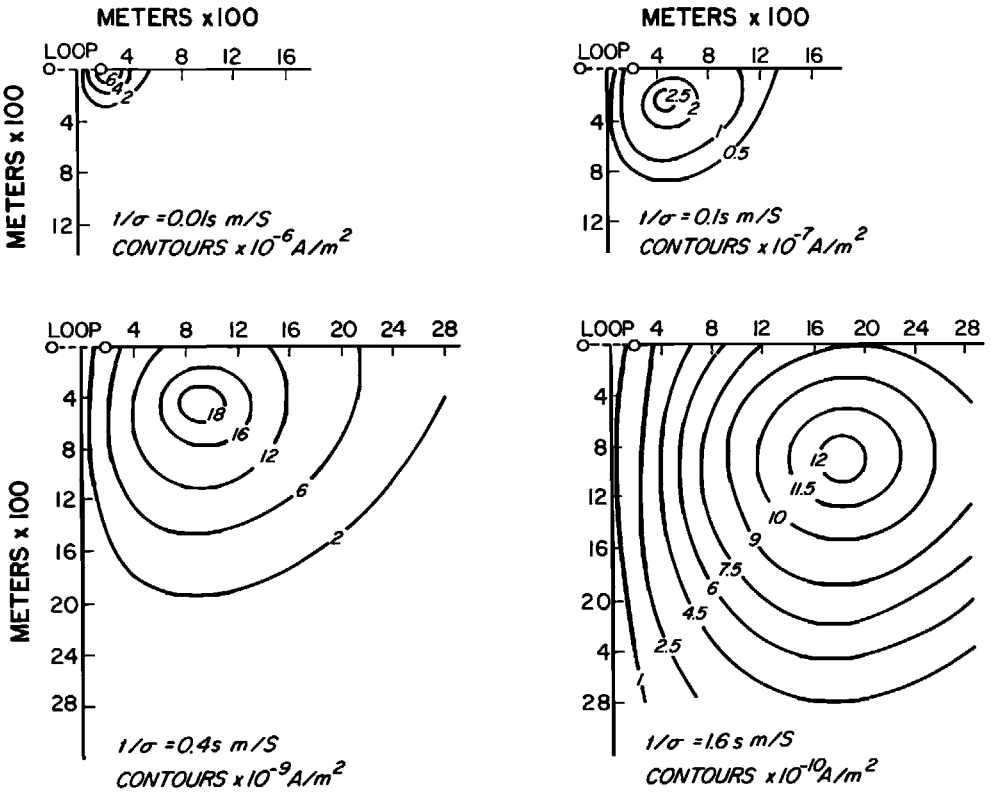

Fig. 19. Contours of the current density in the "smoke ring" of current induced in a uniform conductive half space by a step transient current in a horizontal transmitter loop. Four snapshots in time are provided. The induced current is flowing azimuthally around the vertical axis of the loop, i.e., normal to the plotted section (after Nabighian, 1979).

for EM surveys as loops. However, EM effects are frequently seen in IP surveys, so this case is very important. We must also calculate the field of a buried current source in a later section where the effect of a conductive host region on the EM response of a local conductor is considered.

The magnetic field of a current-carrying grounded wire on a half-space is somewhat complicated in the active region. However, the field in the near zone is relatively easy to calculate using dc resistivity concepts. In either case, taking account of the diffuse current in the ground as well as the current in the source wire is required and this can be difficult. But, for the near zone (static) case of a current source in or on a horizontally layered half-space, Ampere's law provides a convenient trick to avoid finding the exact form of the earth currents. As is illustrated in Figure 21, the source current and the diverging earth currents at each end may be turned into continuous current systems by adding canceling pairs of vertical current lines from infinite depth to the system. Due to the axial symmetry and the fact the no current flows above the surface, Ampere's law shows that the earth currents with their attached current lines contribute nothing to the surface magnetic field. Put another way, the above surface magnetic field of the earth current from one end of the source current is identical to that of a vertical line current from the surface to infinite depth so, as far as concerns the above surface magnetic field, the total current system is equivalent to an infinite buried vertical rectangular loop with an upper edge formed from the source current line and vertical edges projecting deep into the earth from the grounding points.

The magnetic field of an infinite line current is azimuthally directed and axially symmetric, i.e.,

$$H_\theta = \frac{I}{2\pi\rho} \tag{57}$$

where ρ is the distance from the current line.

According to symmetry and the Biot Savart formula [equation (19)], the field of a half-infinite wire in the radial plane containing the end point is half of this. The field produced by a horizontal source wire exclusive of

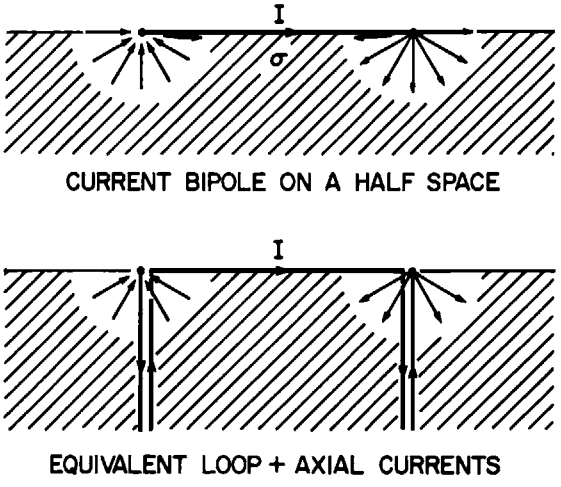

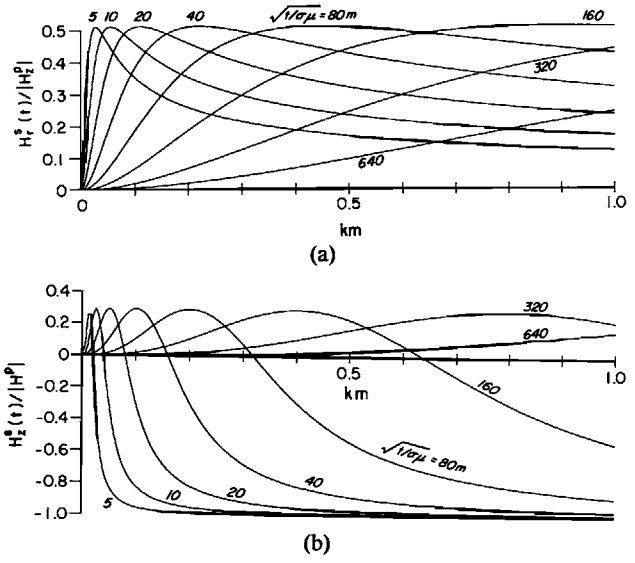

Fig. 20. (a) The normalized secondary magnetic field at the surface of a uniform half space after a current step in a small horizontal transmitter loop (a) radial component (b) vertical component (courtesy of B. Polzer).

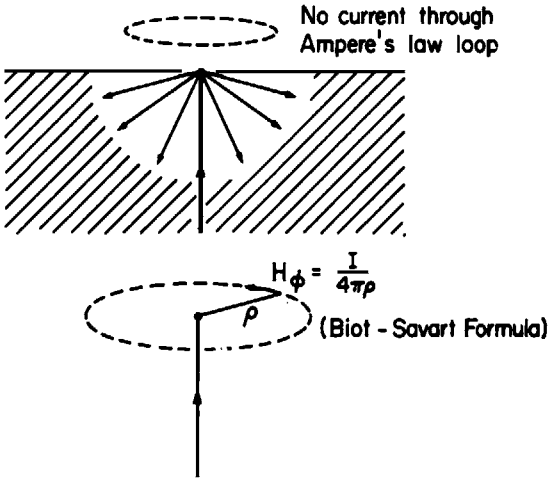

Fig. 21. The magnetic field of a grounded source can be decomposed into three parts, the field of the current line along the surface and the fields of the earth currents at each end. At the earth's surface, the field of an axially symmetric earth current is identical to that of a semi-infinite vertical wire.

the ground currents is also obtainable from the Biot Savart equation. By summing terms for the horizontal segment and the source and sink ground currents, we obtain the total magnetic field of a static horizontal grounded wire system. Note that the ground currents contribute only to the horizontal magnetic field, whereas the wire (if it lies directly on the ground surface) contributes only to the vertical field on the surface. A somewhat surprising corollary of this derivation is that the static magnetic field in the air depends only on the radial symmetry of the source and sink ground currents and is completely insensitive to horizontal stratification in the ground.

To give some idea of the induction effects which take place around a grounded source, the transient step response of the electric and magnetic fields on a half-space are illustrated in Figure 22. In a uniform half-space, there can be no charge distributions anywhere except at the ends of the source wire that might contribute a time-varying component of the electric field. The E transient is therefore produced only by the magnetic field of the wire and thus is always parallel to the wire. Note that there are, however, anomalous E fields perpendicular to the wire with instantaneous (in the quasi-static limit) rather than transient changes in amplitude.

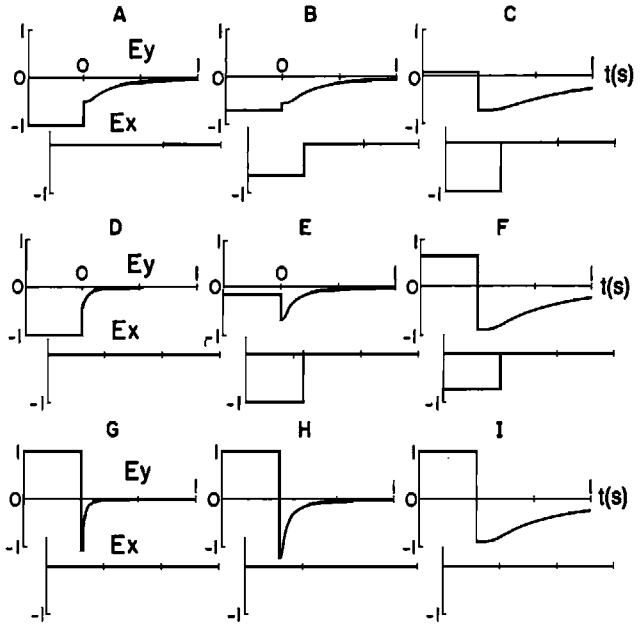

ELECTRIC FIELD TRANSIENTS-HALFSPACE CASE

(a)

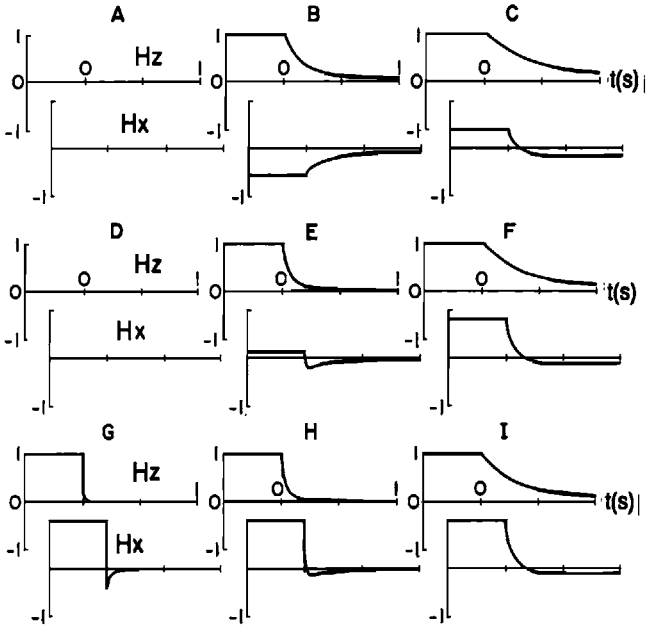

MAGNETIC FIELD TRANSIENTS-HALFSPACE CASE

(b)

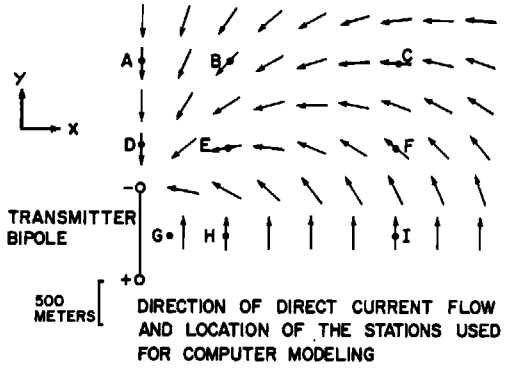

(c)

Fig. 22. Transient electric and magnetic fields on the surface of a uniformly conductive half space at various positions following cutoff in a grounded bipole source (Eadie, 1981).

MODELING INDUCTION IN LARGE ISOLATED CONDUCTORS

Whenever magnetic source EM is used to locate highly conductive zones in very resistive host rocks, only the eddy currents within the conductive materials will be of appreciable amplitude. Then we can neglect any complications caused by the possibly complicated resistivity structure of the host medium and consider the conductive body as if it were in free space. We discussed such cases in previous sections and the basic physics is straightforward. However, for quantitative interpretation of field data, we must be able to model quantitatively a variety of conductor shapes. We must also take account of the coil configuration of the EM system. Unfortunately, there are few conductor geometries for which the induction equations can be solved analytically for a general source field. Much of the past modeling done in support of practical EM interpretation has had to be carried out by means of laboratory scale model measurements. Recently, numerical modeling has been successfully employed to give some practical results.

A conceptual framework for analyzing "conductor in free space" induction problems can be obtained by generalizing the circuit model given in the Eddy Currents in an Ideal Circuit section. We begin by noting that virtually any finite sized vortex of eddy currents may be decomposed into a set of predetermined current patterns of fixed geometry (called a basis). The system then is analyzed as if the elements of the basis were a set of simple loop currents whose mutual inductances are taken into consideration along with their self inductances and resistances. Interaction does not greatly change the algebraic form of induction equations from what was discussed previously, except to give them a matrix form, viz,

$$(\underline{\mathbf{R}} + i\omega\underline{\mathbf{L}})\mathbf{I} = \underline{\mathbf{Z}}\,\mathbf{I} = -i\omega\underline{\mathbf{L}}_t\underline{\mathbf{I}}_i \qquad (58)$$

where $\mathbf{I}$ is an $n \times 1$ vector of the currents I_k in each loop, and the $n \times n$ matrices, $\underline{\mathbf{L}}$, $\underline{\mathbf{R}}$, and $\underline{\mathbf{Z}}$ have elements such that

$$Z_{jk} = R_j\delta_{jk} + i\omega L_{jk}.$$

The indices j and k index the n elements of the current basis so that L_{jk} is the mutual inductance between current paths j and k; R_j and L_{jj} are the resistance and self inductance of the jth loop; L_{jt} is the mutual inductance between current path j and the transmitter and is an element of the $n \times 1$ vector $\mathbf{L_t}$; and I_t is the transmitter current. The matrix $\underline{\mathbf{R}}$ is real and diagonal, $\underline{\mathbf{L}}$ is real and symmetric, and $\underline{\mathbf{Z}}$ is complex and Hermitian symmetric. The vector $\mathbf{L_t}$ is real and $\mathbf{I}$ is complex. I_t is a scalar.

The formal solution of equation (58) is just

$$\mathbf{I} = -(i\omega I_t)\underline{\mathbf{Z}}^{-1}\mathbf{L_t}. \qquad (59)$$

If we then consider the mutual coupling of each current element in the earth to a receiver of an EM system via mutual inductances L_{rj} of vector $\mathbf{L_r}$, we can write the normalized system response in a form analogous to equation (43) as

$$e^s/e^p = -[\mathbf{L}_\mathbf{r}^T(i\omega I_t)\underline{\mathbf{Z}}^{-1}\mathbf{L_t}]/(L_{rt}I_t). \qquad (60)$$

Equation (60) has a very interesting form if an eigenfunction decomposition is performed. We may then write

$$e^s/e^p = -\{\mathbf{L}_\mathbf{r}^T\underline{\mathbf{U}}\underline{\mathbf{S}}\underline{\mathbf{U}}^T\mathbf{L}_t\}/L_{rt} \qquad (61)$$

where $\underline{\mathbf{U}}$ is the eigenvector matrix of $\underline{\mathbf{L}}$ and $\underline{\mathbf{S}}$ is a diagonal matrix

$$\underline{\mathbf{S}} = \left|\frac{\delta_{jk}}{L_j'}\left(\frac{i\omega\tau_j'}{1 + i\omega\tau_j'}\right)\right|$$

where the quantitites L_j' and τ_j' are the jth eigenvalues of the matrices $\underline{\mathbf{L}}$ and $(\underline{\mathbf{R}}^{-1}\underline{\mathbf{L}})$, respectively. The significance of equation (61) is perhaps better appreciated by writing it out as a summation

$$\frac{e^s}{e^p} = \sum_{j=1}^{n}\left[\left(\frac{L_{rj}'L_{tj}'}{L_j'L_{rt}'}\right)\left(\frac{i\omega\tau_j'}{1 + i\omega\tau_j'}\right)\right] \qquad (62)$$

where

$$L_{rj}' = \sum_{k=1}^{n} L_{rk}U_{kj},$$

$$L_{tj}' = \sum_{k=1}^{n} L_{tk}U_{kj}.$$

Comparing equation (62) with equation (43) we see that the primed symbols act just like the mutual and self inductances and time constants of n isolated (non interacting) simple circuits.

The foregoing shows that we can, in general, find n sets of n basis current paths wherein the sets are totally independent of one another. Each set is collectively called an eigencurrent. Currents in the elements of the basis that have the same phase and have amplitudes that are proportional to the elements of one eigenvector have no mutual coupling (mutual energy) with any other eigencurrent. The voltages induced by an eigencurrent flowing in the basis elements are also in phase and proportional in amplitude to the eigenvector, so they serve only to sustain the eigencurrent which generates them. Thus, an eigencurrent set behaves collectively as if it were a single current flowing

in a single isolated circuit. Each eigencurrent has a distinct time constant and self inductance associated with it. The values of these will, in general, be different from those of any of the individual basis elements alone.

The idea of representing the current flow pattern induced in a conductor by an arbitrary source field as the sum of current systems having known geometry is a powerful one that can be applied both in analytical and numerical modeling. To understand how the current pattern evolves with changing frequency (or time) if the basis of the decomposition is a set of eigencurrents, is particularly easy because of their simple circuit-like spectral or time response. If the induced current pattern at the inductive limit is decomposed into eigencurrents, we see, for instance, that the response in the resistive limit is given by the same sum but with the terms reweighted by the inverse of their time constants. The time domain step current response is analogous. The induced current immediately following the step has the same form and eigenfunction decomposition as the inductive limit response in frequency domain. The induced current at a latter delay time is just the same sum but with the terms rescaled according to the time decay of each eigenfunction ($\exp -t/\tau_j$). We see immediately that the eddy current system eventually takes the form of the eigenfunction with the greatest time constant.

To consider an example, a numerical algorithm was created by Annan (1974) for computing eddy current induction in a thin rectangular plate. First, a set of numerically described basis currents is set up using polynomials. The interaction matrix is then set up and eigencurrent density distributions are found (unique to a plate of given length-to-width ratio) along with the time constant and self inductance of each (from the eigenvalues). Then the mutual inductances between each of the eigencurrents and the source and receiver are calculated and combined according to the loop equations (62) to give the response of the plate to a given EM system. In theory, an infinitely large set of eigencurrents is required to represent exactly the induced currents in a continuous conductor, but reasonably accurate results can often be obtained with a small number of terms in the summation. In the 1981 version of the computer program implementing Annan's algorithm, only 15 eigencurrents can be used and these have only a comparatively small range of time constant (<5:1). Figure 23 shows a set of eigencurrents for a 2 × 1 plate. The small number of terms means that cases where the receiver and transmitter are close to the plate (relative to the plate dimensions) cannot be simulated accurately because the limited set of eigencurrents cannot represent a current system that is strongly localized in a small part of the plate. Nevertheless, the modeling program is a most useful interpretational aid.

The sphere is the only shape which has been widely used for analytical modeling purposes, and is a good basic model for compactly shaped conductors. Numerous variants have been treated: various source field configurations, transient and spectral response, radially varying conductivity, changing permeability, etc. In all solutions, the induced eddy currents are decomposed into components which have related patterns. The primary classification is by the external magnetic field (according to the multipole moment from which it is generated). The secondary division is into current systems producing the same external multipole field, but configured inside the sphere so as not to interact with each other. Each is thus an eigencurrent and there is an infinite number for each multipole component, each having a slightly different time constant and amplitude coefficient. All eigencurrents of the same multipole order couple to the primary field in the same way, and thus for all geometric purposes, the currents for each multipole order can be treated as a group having a total spectral response governed by the pole (time constant) distribution of the eigencurrents. A characteristic of a finite body is that the time constants of the eigencurrents are distinct and there is an upper bound to the time constants in each multipole set (Nabighian, 1970, 1971).

Figure 24 shows in (a) the spectral responses of the lower order induced multipoles in a nonmagnetic sphere of uniform conductivity and in (b) the corresponding step responses. Each of the spectral responses is a sum of many eigencurrents and thus is somewhat more smeared out than is the response of a single loop. The time domain decays have a visibly nonexponential form at early time. There is also a clear tendency for the range of time constants that contribute appreciably to each to shift systematically to smaller values as the multipole order increases. The high order terms become more important near the inductive limit (in frequency domain) or at early time (in time domain).

If the sphere is magnetic (i.e., its relative permeability μ/μ_o is appreciably greater than 1), there are two changes from the nonmagnetic case (Figure 25). First, the time constants of the eigencurrents increase with increasing permeability. Second, at low frequency, an additional magnetic moment is created in the sphere which has an opposite sign to the induction moment. The magnetic moments strength is in proportion to the magnetic susceptibility and the internal field intensity and tends to increase the magnetic flux density inside the body. As frequency or conductivity is increased, the eddy currents flow so as to reduce the internal magnetic flux density until the density vanishes at the

inductive limit. Thus the moment due to eddy currents can overpower the magnetic effect, so the same inductive limit is reached irrespective of magnetic permeability.

The number of multipole terms needed for accurate representation of induction in a sphere depends on the convergence of the summation. The coefficients of the terms depend strongly on the radial distance of the source and observation point in relation to the radius of the sphere. If the source and observation point are more than about one sphere radius a away from the sphere surface, the first (dipole) moment will strongly predominate. On the other hand, if both are close to the surface (say $<0.1a$), a very large number of moments will be required in the series, and the main part of the observed response will come from the higher order moments. In the former case, the contribution from the eigencurrent of longest time constant (which is part of the dipole term) will be a large part of the total response but will not be in the latter case. The observed response will then be characterized by a broad, almost continuous spectrum of time constants.

Because of the spherical symmetry, induction in a sphere is triply degenerate. Therefore, the same pattern of eigencurrents and time constants can exist about any of the three cartesian axes (or in any orientation). They will not exist, however, if the conductor is less isotropic. At the other extreme from a sphere is a thin conductive plate in which eddy currents can circulate only in the plane of the plate so there is only one set of eigencurrents. In an intermediate case like an oblate spheroid or slab, the eigencurrents which flow normal to the smallest principal axis will have both longer time constants and (generally, because of their larger area) larger mutual inductances with the source and receiver than eigencurrents oriented in other directions. Observation techniques which reveal how the induction changes its strength and time constant with orientation can be very helpful in the interpretation of conductor geometry.

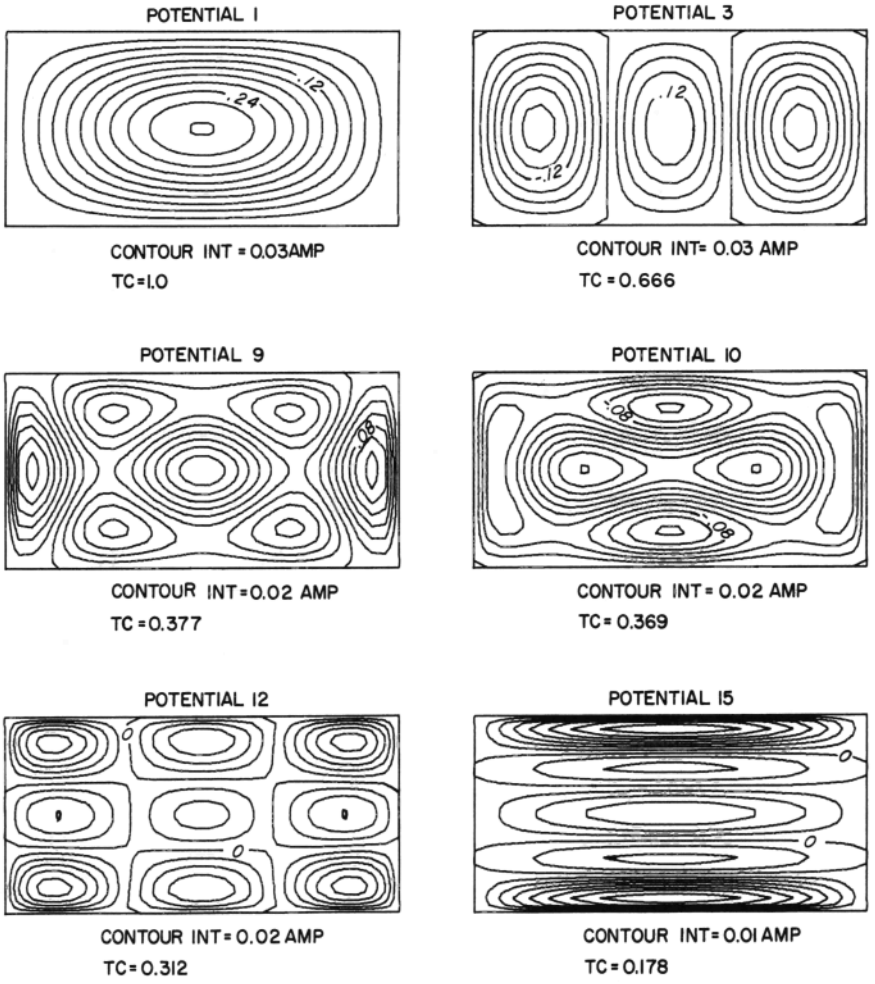

Fig. 23. Streamlines of some of the principal eigencurrents that can be induced in a thin (2×1) conductive plate (from a set of 15) (after Annan, 1974).

Much EM interpretation has been based on a dipping, conductive, infinite, half-plane because only a few parameters are required to describe the model (depth-to-top, dip, surface conductivity). There is now a computing algorithm for calculating time domain induction by a dipole source in such a conductor (Weidelt, 1983), but most interpretational material in the literature has been obtained by scale modeling. It has long been possible to compute the inductive limit response for an arbitrary source configuration. Figure 26 shows a comparison of spectral responses from a half-plane model and a small plate. Because there is no fixed limit to the size of the eddy current vortex that can be induced in a half plane, the low-frequency response has a slower frequency dependence (in the measurable range) than a loop or other confined conductor (Kaufman, 1978). Because of the half-plane's infinite extent, its eigenfunctions are neither discrete nor of bounded time constant. The spectrum of time constants is continuous and unbounded. Thus, the transient response at late time never becomes exponential but follows an inverse power law instead.

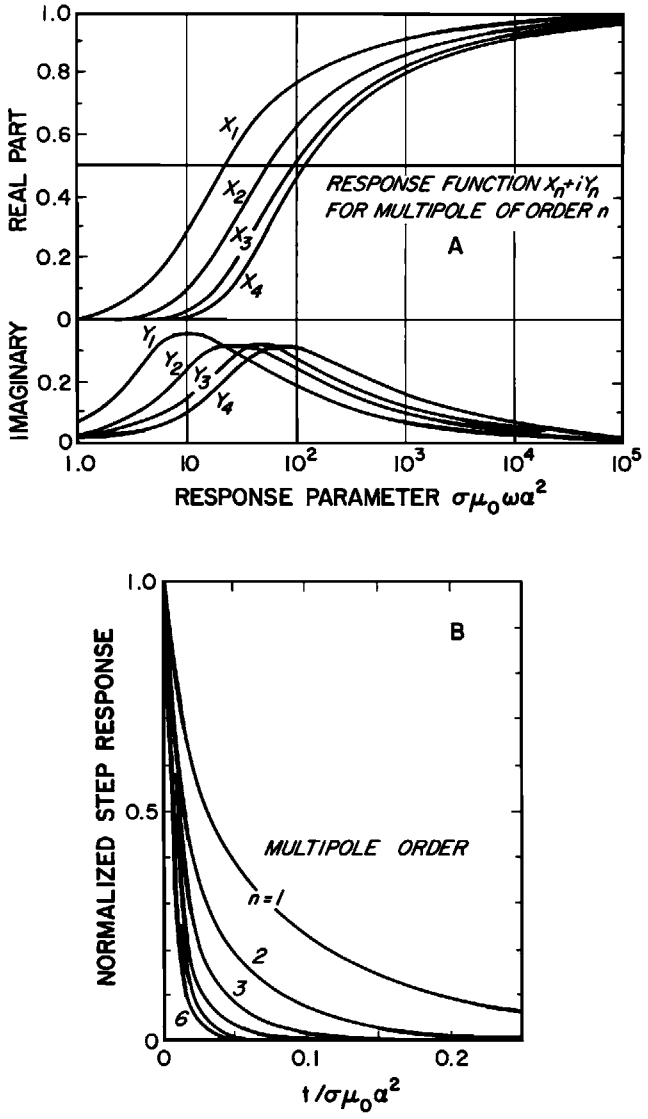

Fig. 24. (a) Spectral response and (b) transient response of the multiple moments induced in a uniformly conductive sphere by a nonuniform primary magnetic field (after Nabighian, 1970, 1971).

A related case that can be easily solved analytically, and one that is very useful for representing a conductive overburden, is the transient response of an infinite thin sheet. The secondary magnetic field response to a local magnetic source undergoing a step change in intensity is exactly represented as the field of an image source created behind the sheet at the step instant, after which it moves away from the sheet at a constant velocity $z/t = 2/(\mu\sigma s)$ (s = thickness of sheet). This leads to a t^{-3} late time fall-off in the vertical magnetic field corresponding to a continuous and unbounded set of time constants in the response as expressed in equations (62).

The models discussed are often used to represent conductive mineralization. All models are of uniformly conductive bodies. However, we know that sulphide mineralization is often extremely heterogeneous. On a small scale, even relatively massive mineralization is an interconnected network that includes a substantial percentage of insulating gangue minerals, and on a larger scale, we usually find that the tenor of a mineralized zone is anything but uniform. Often, a less highly mineralized halo will surround at least part of the core mineralization. Although we are far from modeling quantitatively the effects of such inhomogeneity, clearly there is a highly visible influence on spectral response, just as stranding or spacing of the wire in an inductor can have an important influence on the high-frequency impedance. The main effect is to broaden the response spectrum, particularly near the inductive limit. Otherwise stated, the distribution of time constants among the eigenfunctions of an inhomogeneous conductor will be extended and emphasized in the direction of short time constants in comparison to that of a similarly shaped homogeneous conductor. If a model with uniform conductivity is used to interpret data from an inhomogeneous conductor, we will find that the interpreted conductivity increases systematically with decreasing frequency (or increasing decay time). Figure 27 shows horizontal loop EM (Slingram) data over a sulphide body which shows the effect very clearly. In resistive terrain where the inductive response of the subsurface conductor can be accurately determined to high frequency, this dispersion in interpreted conductivity is

so regularly observed over sulphide mineralization that it has diagnostic value.

EFFECT OF A CONDUCTIVE OVERBURDEN

The overburden and host rock in some parts of the Baltic and Canadian Shields are often so poorly conductive that they can be neglected totally in EM modeling. But this is rarely the case elsewhere, so we must necessarily consider their effects. If they are sufficiently conductive, clearly the EM system will respond to them as was discussed in a previous section. However, the response of an anomalously conductive zone in a conductive earth is not just the sum of the responses of the host medium and the anomalous conductor taken separately. They respond jointly. Nevertheless, we may often be able to distinguish between the two on an EM profile or map, because the anomalous conductor will produce a local anomaly which is superimposed on a broader background response from the host earth.

In discussing how a conductive overburden or host rock affects the local (stripped) response of a local target conductive zone, we shall assume that if the earth as a whole is appreciably conductive, it is laterally uniform and very extensive in comparison to the target conductor and can therefore be modeled as a horizontally layered structure. We shall then determine the effect which the conductive overburden and host rock have on the residual response of the target, taking the free-space response of the target as a baseline for comparison.

Often, overburden is much more conductive than the bedrock in which the target conductor is likely to be situated. If the immediate surroundings of the target are insulating, the effect of a conductive overburden interposed between the EM system and the target is relatively simple. The magnetic field of the source is somewhat altered from its free space form in passing downward through the overburden to the target, and the secondary field of the target will be similarly modified in passing upward to the receiver. The effect can be likened to the action of a low-pass frequency filter or transfer function. Unless the overburden is extremely conductive so there is a very strong attenuation, the direction of the field is little changed and the amount of filtering is similar everywhere in the target zone. The characteristics of the filter can be estimated roughly from equation (37). The primary field from the source and the secondary field generated by the target usually are localized fields such as were

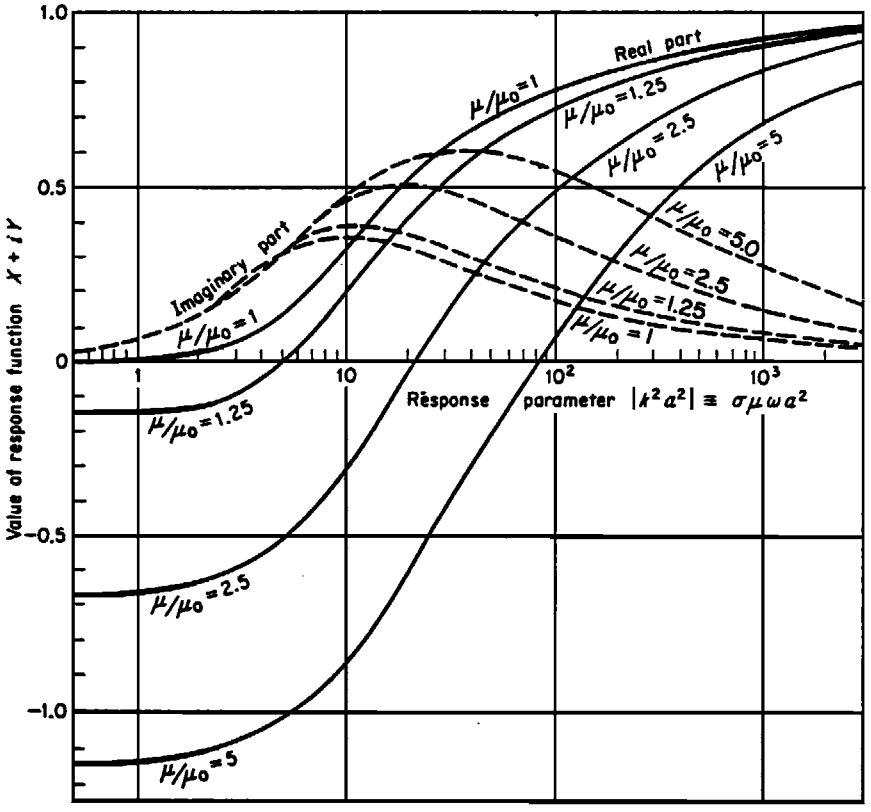

Fig. 25. Spectral response of a permeable conductive sphere in a uniform alternating magnetic field (after Wait, 1951a).

discussed in equation (37) and to which we may ascribe a horizontal scale parameter l ($= \lambda^{-1}$) which characterizes the region encompassing the source and the receiver point and the significant parts of the target conductor. For passage of the fields both ways through an overburden of thickness h, the transfer function will take the form

$$T_0 = \exp\left\{\left[1 - \left(1 + \frac{2il^2}{\delta_0^2}\right)^{1/2}\right] 2\,\frac{h}{l}\right\}$$
$$= \exp\left\{\left[1 - \left(1 + i\beta_0\,\frac{l^2}{h^2}\right)^{1/2}\right] 2\,\frac{h}{l}\right\} \qquad (63)$$

where $\beta_0 = \sigma_0 \mu \omega h^2$.

As frequency is raised such that the skin depth in the overburden δ_0 becomes comparable or small relative to h, [equation (63)] becomes vanishingly small as

$$T_0 \rightarrow \exp - [2(1 - i)h/\delta_0] \qquad (64)$$

and the primary and secondary fields will hardly penetrate the overburden and negligible target response will be observed. On the other hand, the overburden will have no effect at very low frequency but then there may not be much response from the target either. In the middle range where the overburden skin depth is finite but substantially greater than l, the situation referred to in equation (39) arises, and the transfer function will become

$$T_0 \approx \exp - (ic\sigma_0 \mu \omega l h) = \exp - (ic\beta_0 l/h). \qquad (65)$$

An unspecified free constant c (≈ 1) has been inserted in this expression to take account of the arbitrariness of the scale factor l. This transfer function is a phase shift proportional to frequency which rotates the anomaly phase angle toward (or past) the free space inductive limit. Once the phase shift becomes large

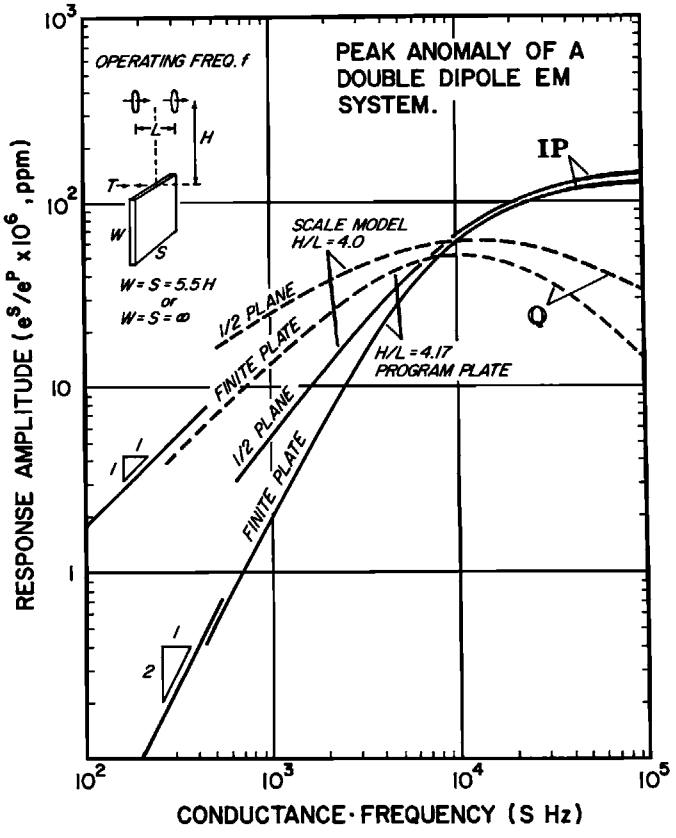

Fig. 26. Spectral response of a half plane compared with the spectral response of a small plate, for a double dipole EM system over the edge of the conductor (after Lamontagne, 1975).

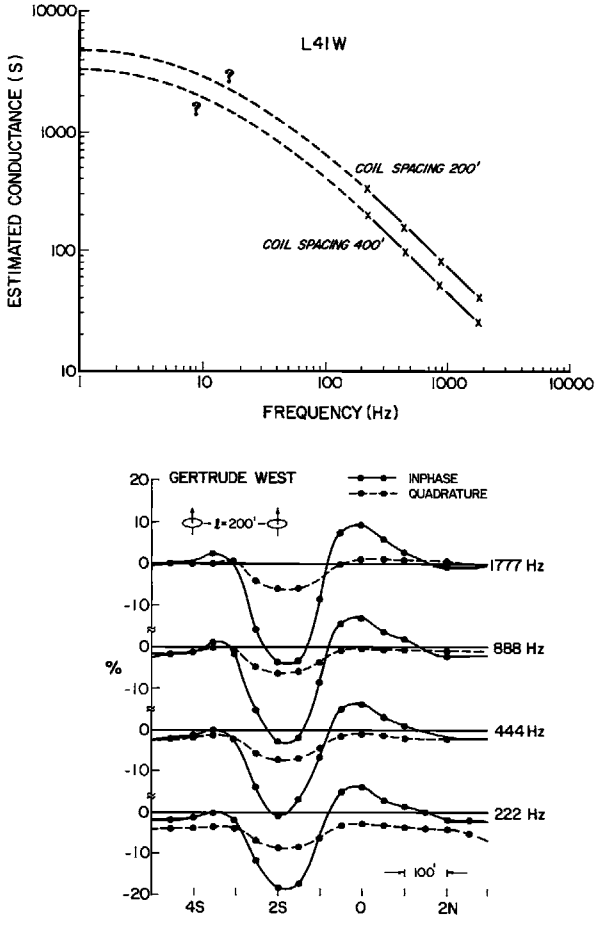

Fig. 27. EM response observed over a massive sulphide zone at four frequencies. When the observed spectral response is matched, frequency by frequency, with any simple uniformly conductive model, the fitted conductivity rises with decreasing frequency. The effect is large unless the induced response is in the resistive limit, i.e., the ratio of in-phase to quadrature response is well below one (HLEM data by courtesy of J. Betz and INCO Limited).

(≈1 radian = 57°), we must revert to the more accurate form [equation (63)] and we find that the amplitude attenuation begins to become very noticeable. Basically, the overburden acts as a low-pass frequency filter; which has a linear phase-frequency characteristic in the spectral region just below the cutoff frequency.

The EM response of the overburden itself (i.e., of an earth without the target conductor) can be thought of as a reflection response, and its spectral form R_0 will be approximately the complement of the transmission response discussed, i.e., $R_0 = (1 - T_0)$. The amplitude A_0 (i.e., the inductive limit response) will depend on the position of the receiver and transmitter relative to the overburden and might be estimated using image concepts. In the case of a horizontal coil transmitter and receiver, A_0 is just the negative of the free space primary coupling. If we then approximate the free space response of the target conductor by a single pole and zero response as in equation (47), we are in a position to write an approximate representation for the total EM response of the target and the overburden together.

$$\frac{e^s}{e^p} = -T_0(\beta_0, l/h)A_b\left[\frac{i\gamma}{1 - i\gamma}\right] - R_0(\beta_0, l/h)A_0 \qquad (66)$$

where $\beta_0 = \sigma_0\mu\omega h^2$, $\gamma = i\omega\tau_b$, A_0 is a geometrical factor describing the normalized high frequency (inductive limit) response of the overburden and, as in equation (49), A_b is the normalized inductive limit free space response of the target body

$$A_b = -(G_{tb}^{Hm}\, m_{bL} G_{br}^{Hm})/G_{tr}^{Hm},$$

where $m_{bL} = V/(1 - N)$.

Figure 28 illustrates this by showing in a phasor plot the local (stripped) response of a vertical plate target conductor under a conductive overburden as computed by a full numerical modeling method. Figure 29 shows a field case where the horizontal loop response from a steeply dipping conductor in an insulating unweathered Precambrian bedrock is phase shifted by the conductive overburden.

The effect, in time domain, of a conductive overbur-

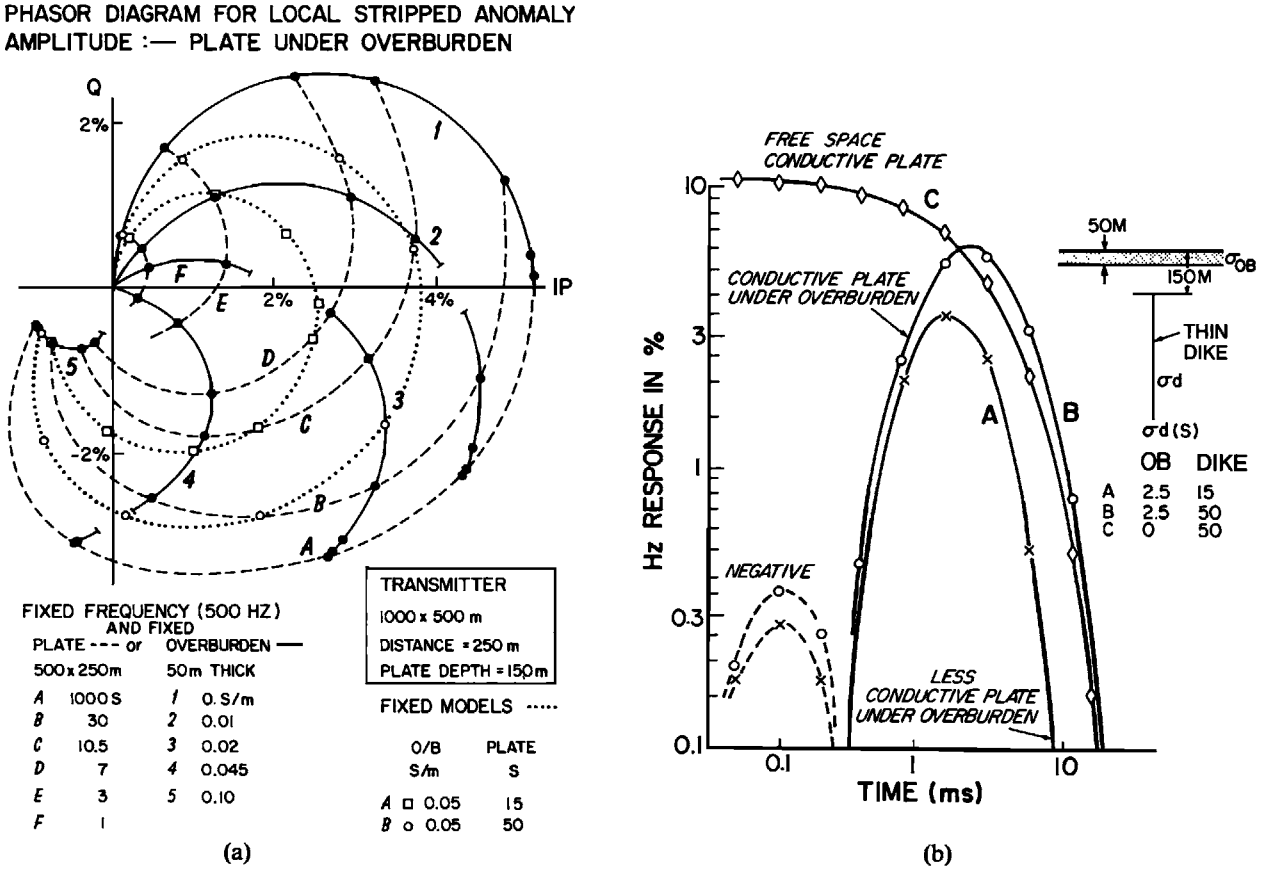

Fig. 28. (a) An example of the effect of a conductive overburden on the stripped frequency-domain response of a target conductor beneath it, obtained by numerical modeling (Lajoie and West, 1976) and (b) the stripped time domain step response as transformed from the frequency domain results (West et al., 1984).

den on changing the local, residual response of a target conductor from the conductor's free space form is also quite simple. Transformed to time-domain, the first term of equation (66) is a convolution of the overburden's pulse transmission response with the free space target response. The secondary magnetic field response of a target in free space to step discontinuity in transmitter current is a simple exponential decay, as given in equation (44)

$$\frac{H^s(t)}{H^p(0)} = -[T_0(t) * A_b u(t) \exp -(t/\tau_b)] - [R_0(t)A_0]. \quad (67)$$

where $T_0(t)$ and $R_0(t)$ are the Fourier transforms of T_0 and R_0.

The overburden transmission filter in equation (63) is a little difficult to transform, but for heuristic purposes and when the overburden conductivity is not great, it too can be roughly modeled as a circuit whose response is the complement of a single pole and zero loop response with time constant τ_0

$$T_0 \approx \left(\frac{1 - i\omega\tau_0}{1 + i\omega\tau_0}\right)$$

$$R_0 \approx \left(\frac{i\omega\tau_0}{1 + i\omega\tau_0}\right). \quad (68)$$

The transforms of T_0 and R_0 then also consist of a simple exponential having a decay constant τ_0

$$T_0(t) \approx [1 - \exp -(t/\tau_0)]u(t)$$

$$R_0(t) \approx u(t) \exp -(t/\tau_0). \quad (69)$$

Convolution of the overburden filter with the target body's free space response then just blunts the onset of the transient and delays the overall response an amount τ_0, i.e., a finite rise time of order τ_0 is introduced on the target response. For example in Figure 28, τ_0 is about 1 ms, and the delay at times >2 ms is easily seen (curve B) when compared to the free-space response (curve C). The late-time difference between curves B and C should thus not be

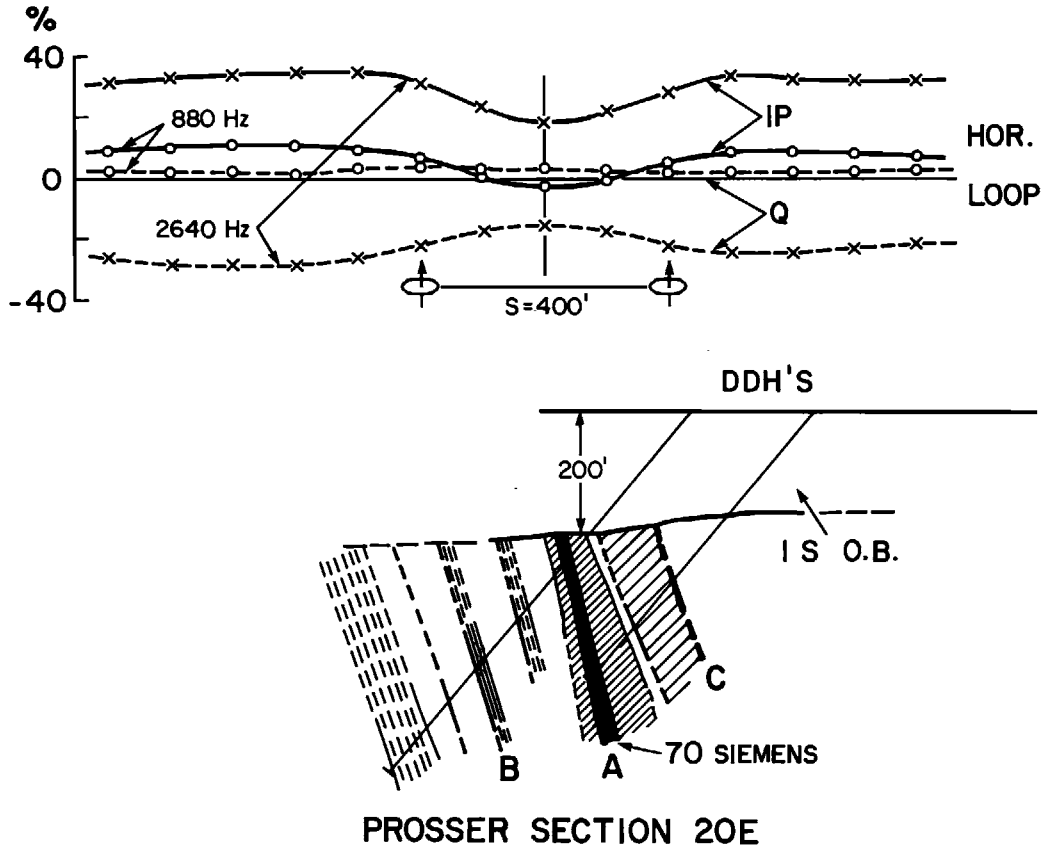

Fig. 29. A field example of a slingram (HLEM) survey over a graphitic conductor in resistive bedrock showing phase rotation by the overburden (courtesy of J. Betz).

regarded as an amplitude enhancement at equal delay time. The more accurate filter function of equation (63) can be transformed, the only difference is that the transmitted pulse itself is predicted to have a blunt beginning. However, the effect on the overall response is little different from that of equation (69).

Since the secondary magnetic field generated directly by the overburden layer [corresponding to the second term in equation (66)] has basically the same frequency response as transmission through the overburden, the time domain form of response to a step current in the transmitter will be essentially a decaying transient with about the same time constant as the transmission response. At early times (relative to τ_0), the primary field is mainly reflected back upward, whereas at later time, it penetrates through the overburden suffering only a little delay and blunting. When it reaches the target body, a secondary response is excited, which then must be transmitted back to the surface which causes blunting and further delay. Obviously, if the time constant for double transmission through the overburden is long compared to that of the target body, the target will be invisible to a surface EM system.

TARGET CONDUCTOR IN A CONDUCTIVE HOST

A conductive host medium surrounding and in contact with the target body has a more complicated effect on EM response than does an isolated overburden, although there are some common features. This problem is difficult to analyze theoretically because of a lack of appropriate coordinate systems in which to describe the geometry of the conductors. Numerical methods of solving integral equations for the EM field have been used to make fairly comprehensive studies of the response of a vertical plate target in a conductive host to Turam and Slingram EM systems (Hohmann, 1988; Hanneson and West, 1984). A few cases where the target is a three-dimensional block have also been studied numerically. Analog model studies of other conductor geometries and other configurations of the EM system show characteristics similar to the numerical models.

The basic novel element in the physics of EM induction when a conductive host is present is that a second type of current flow can produce a secondary magnetic field, in addition to the closed vortex type of current circulation that is induced in a conductive body in free space. The situation is sketched in Figure 30. The additional pattern is a current flow which passes through the boundary of the target. We shall refer to this flow as a galvanic current because it enters the target body by direct contact with the host medium. For a magnetically coupled (loop-loop) EM system, the source of galvanic current in the host medium is the regional scale induction, i.e., those induced currents that produce the host medium's background EM response, as discussed previously. In analyzing the galvanic current flow pattern due to the presence of a local target body, we consider the current density in the ground to be made up of two parts, a primary current density which is what would exist if no target body were present, and a secondary component due to the body's presence which is the aforementioned galvanic flow. Then, following the procedure discussed in an earlier section, the galvanic flow will be considered to be generated by an anomalous current flowing in the host material and confined within the target zone. The anomalous current density J_a is related to the primary current density J^p in the host medium, the relative ohmic susceptibility κ_σ of the body, and to the shape of the body relative to the direction of current flow (represented by the shape depolarization factor of the body in the direction of J^p). Its strength is limited by the depolarization phenomenon, i.e., by the charge which arises on the boundary of the conductor. From equations (26) and (28)

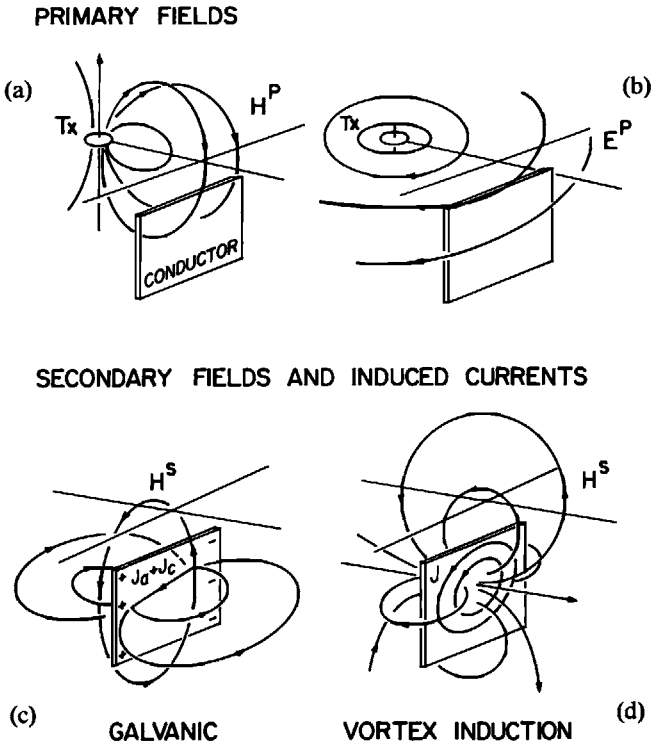

Fig. 30. Sketches of galvanic and vortex induction in a conductive zone. (a) primary magnetic field, (b) primary electric field, (c) induced galvanic current flow and its associated secondary magnetic field, (d) induced vortex current flow and its secondary magnetic field.

$$J_a = \frac{\kappa_\sigma \sigma_h E^p}{(1 + N\kappa_\sigma)} = \frac{\alpha}{(1 + \alpha)} \frac{J^p}{N} \tag{70}$$

where $\alpha = \kappa_\sigma N$ is the normalized channeling number of the target conductor. The total electric current dipole moment of the body is then

$$j_b = VJ_a.$$

Just as the toroidal induction vortex configures itself so that its secondary magnetic field tends to cancel the primary magnetic field in the target body, the primary and galvanic current circulations together produce a charge distribution on the surface of the target body which in turn creates a secondary electric field that tends to cancel most of the primary electric field inside the target body. The charge concentration arises nearly instantaneously, so the frequency dependence of the galvanic current system is essentially that of the primary electric field in the target area. Skin effect in the galvanic current may modify this picture to some extent, but only if the target is very conductive and depolarization is minimal. We shall neglect this complication here, as it only arises in special cases.

The nature of the primary electric field produced by the EM transmitter in the host medium was discussed in previous sections. For the moment, we shall consider only the case where the overburden and host rock are insufficiently conductive to attenuate the electric field much in comparison to the resistive limit cases; i.e., the target zone is in the near zone of the transmitter. The near-zone electric field at the body due to an alternating magnetic dipole transmitter m_t always has the form

$$E_b = i\omega\mu G_{bt}^{Em} m_t \tag{71}$$

where G is a pure geometrical factor whose dimensions are (distance)$^{-2}$. For example, the horizontal (azimuthal) electric field in the near zone of a vertical magnetic dipole transmitter of moment m at a cylindrical radius ρ and depth d will be

$$E_\phi = \frac{-i\omega\mu m_i}{4\pi} \frac{\rho}{(\rho^2 + \alpha^2)^{3/2}}. \tag{72}$$

The galvanic current system set up by E_ϕ can generate a secondary magnetic field at the surface. We may express the surface magnetic field at the receiver at low frequency, due to a short source current dipole of strength j_b at the center of the target body in the interior of any horizontally layered earth, symbolically as

$$H_r^s = G_{rb}^{Hj} j_b \tag{73}$$

where, as in the case of the electric field of a magnetic dipole, G is a pure geometrical factor with dimensions of (distance)$^{-2}$. However, this is not so simple to evaluate as is the surface magnetic field of a loop current (magnetic dipole) because it is essential to take account of the host space. The problem is familiar from analyzing the magnetometric resistivity method and was discussed in an earlier section. The surface magnetic field of the total current system established by a source current in a horizontally stratified host medium was shown to be like that of an extended rectangular buried loop of current where the source current dipole forms one side and the remainder is completed by two vertical segments to infinite depth.

As an example, the components of the surface magnetic field along a traverse along the x axis due to a horizontal current dipole in the y direction at depth d under the origin are

$$H_z^s = \frac{j_b}{4\pi} \frac{x}{(x^2 + d^2)^{3/2}}$$
$$H_x^s = \frac{j_b}{4\pi} \frac{z}{(x^2 + d^2)^{3/2}}. \tag{74}$$

The form of this is generally similar to the field of an x directed magnetic dipole located at the same point (such as might be produced by vortex induction) except that this is a broader anomaly, because of the weaker distance dependence in these Green's functions (McNeill et al., 1984).

At this point, with V,α, and N defined in equation (28) we can combine equations (71) and (72), include a transmission filter factor for the frequency filtering effect of conduction in the overburden and host rock between the target body and the surface, and write an expression for the normalized anomalous response of an EM system due to the galvanic current system.

$$\left(\frac{e_s}{e_p}\right)_{\text{galv}} = T_{oh}\left\{\left(\frac{G_{rb}^{Hj} G_{bt}^{Em}}{G_{rt}^{Hm}}\right) \times \left(\frac{i\sigma_h \mu\omega V}{N}\right)\left(\frac{\alpha}{1 + \alpha}\right)\right\} \tag{75}$$

where the middle term can be rewritten as $i\beta_h V/Nl^2$ in which $\beta_h = \sigma_h \mu\omega l^2$.

To this result must be added the vortex induction response of the target body as it would occur in free space [equation (49)] and the response of the host rock and overburden.

To roughly quantify the transmission filter in equation (75) we follow the procedure used in the last section where a simple expression was obtained for the filtering effect of the overburden on magnetic fields passing through it, and was used to estimate the vortex induction response of a target body under a conductive

overburden. We can do the same for the galvanic case. The magnetic field of an alternating galvanic source current system will, in general, suffer phase delays and attenuation in reaching the surface, just as the primary electric field will suffer some phase delay and attenuation in reaching the target region from the source. The situation is completely analogous to the modification factor for the magnetic field given in equations (63–65). When the overburden and host rock are conductive but still relatively easily penetrated by the fields, and the transmitter and receiver locations are close to the target body, the filtering factor is just a phase shift

$$T_{oh} = \exp - (2ci\sigma_{oh}\mu\omega ld) \tag{76}$$

where

$$\sigma_{oh} = [\sigma_o h + \sigma_h(d - h)]/d$$

and where d is the depth from surface to significant parts of the target body and h is the overburden thickness. Except for possible minor differences in the geometrical factor c, the same expression will apply to either the induction vortex or the galvanic currents. A more complicated formula could easily be written, based on equation (63), to include the attenuation effects which set in at higher frequencies.

We can therefore write an approximate expression for the normalized response of a small target conductor in a conductive host rock and under a conductive overburden to a loop-loop EM system which takes account of both galvanic and vortex induction currents in the target body and the host response as

$$\frac{H^s}{H^p} = \frac{e^s}{e^p} = T_{oh}(\beta_{oh})\left\{\left[\left(\frac{G_{rb}^{Hj} V\, G_{bt}^{Em}}{G_{rt}^{Hm} N^g l^2}\right) \times \left(\frac{\alpha}{1+\alpha}\right) i\beta_h\right] - \left[\left(\frac{G_{rb}^{Hm}\, V\, G_{bt}^{Hm}}{G_{rt}^{Hm}\,(1 - N^i)}\right) \times \left(\frac{i\gamma}{1+i\gamma}\right)\right]\right\} + A_{oh} R_{oh}(\beta_{oh}) \tag{77}$$

where the G functions are the low frequency normalized Green's functions expressing the geometrical relationship between a field component at one point produced by a dipole moment at another point, T_{oh} is the normalized low-pass frequency filter that expresses the phase shift and attenuation suffered by the primary and secondary fields in being transmitted from surface to depth and back to the surface again, R_{oh} is the normalized spectral reflection response of the ground, and A_{oh} its inductive limit amplitude normalized to the free space primary response. V is the volume of the target body and N^g and N^i are its shape depolarization factors along the axes of galvanic and vortex induction (usually perpendicular to one another). The parameters α, β, γ describe in dimensionless terms the physical properties and property contrasts of the model; i.e., they are, respectively, the target body's normalized current channeling number, the overburden and host inductive response parameters, and the target body's normalized inductive response parameter.

$$\begin{aligned} \alpha &= \kappa_\sigma N^g, \\ \beta_{oh} &= \sigma_{oh}\mu\omega ld, \\ \beta_h &= \sigma_h \mu\omega l^2, \\ \gamma &= \omega\, \tau_b, \end{aligned} \tag{78}$$

l = horizontal scale of the EM system and the target body, d = depth of the body, and h = thickness of the overburden.

The foregoing expression should not to be expected to predict EM response accurately for a given model geometry, but the expression does indicate the form of the response and how the response will change with an adjustment of model parameters. Note that the vortex inductive and galvanic terms in equation (77) have opposite signs. This is simply a consequence of the sign conventions for the G functions. Usually, when the target body is well coupled to the EM system, both terms will contribute in the same polarity.

Figure 31 shows some frequency domain response data for the Turam secondary field anomaly of a plate conductor in a conductive host, calculated using a full numerical model. The results show anomaly generation by both galvanic and vortex induction modes. West and Edwards (1985), show that this data can be almost perfectly reproduced by a simple formula like equation (77) if the geometric and other parameters of the target body are appropriately adjusted and the transmission and reflection factors are computed using layered earth modeling formulas.

Certain parts of the response system have been left out of the above analysis (specifically, the mutual coupling between the galvanic and vortex induced currents and between them and the currents in the host space and overburden). Also shown in West and Edwards (1985) is that in usual situations they have negligible effect on the observed response. This is an important observation, because accounting for these effects is one of the main reasons that full numerical solutions are so computationally laborious. It suggests that much interpretation could usefully be based on approximate solutions that are easier to compute.

One advantage of a simple form like equation (77) is that it can be transformed to time domain quite easily because the frequency dependent parts are clearly identified. The step response will be

$$\frac{H^s(t)}{H^p(0)} = T_{oh}(t) * \left\{ \left[\left(\frac{G_{rb}^{Hj}\, V G_{bt}^{Em}}{G_{rt}^{Hm}\, N^{gl^2}} \right) \times \left(\frac{\alpha}{1+\alpha} \right) \sigma\mu l^2\, \delta(t) \right] - \left[\left(\frac{G_{rb}^{Hm}\, V\, G_{bt}^{Em}}{G_{rt}^{Hm}\,(1-N^i)} \right) \times u(t)\, \exp\,(-t/\tau_0) \right] \right\} + A_{oh} R_{oh}(t) \qquad (79)$$

where

$T_{oh}(t)$ is a delay and smoothing filter for transmission from surface to the conductor depth and back, having an approximate time constant of about τ_{oh}.

$A_{oh}R_{oh}(t)$ is the secondary (reflection) response transient of the host rock and overburden having the important part of its time constant spectrum centered about τ_{oh}.

Figure 32 shows some scale model time-domain magnetic field step responses and also Fourier transformed versions of (Holladay, 1981) Lajoie's data from Figure 31.

We obtain no information about response amplitude just by looking at equation (79), but order of magnitude estimates are easily made by evaluating the G functions for a typical case. Consider a vertical magnetic dipole transmitter at a horizontal distance l from a vertical component magnetic field receiver and straddling a small target conductor whose depth to center is d (Figure 33). The free space inductive coupling terms, G_{rb}^{Hm} (the vertical magnetic field of a horizontal

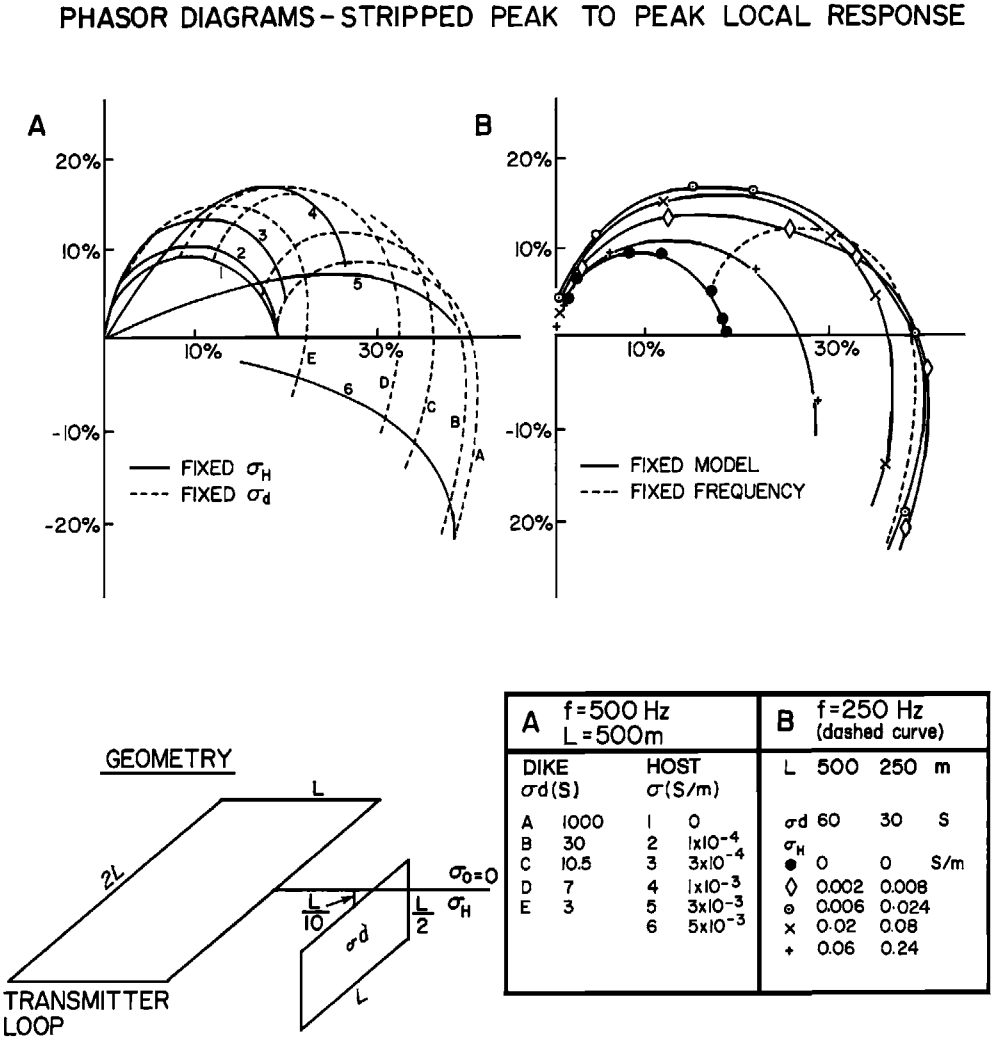

Fig. 31. Computed model data showing frequency domain induction in a conductive plate in a conductive halfspace. The data are shown as phasor diagrams of the amplitude of the local (stripped) anomaly due to the plate. The anomaly from the half-space is not included (after Lajoie and West, 1976). (a) The effect of variations in the conductance of the plate, (b) the effect of halfspace conductivity.

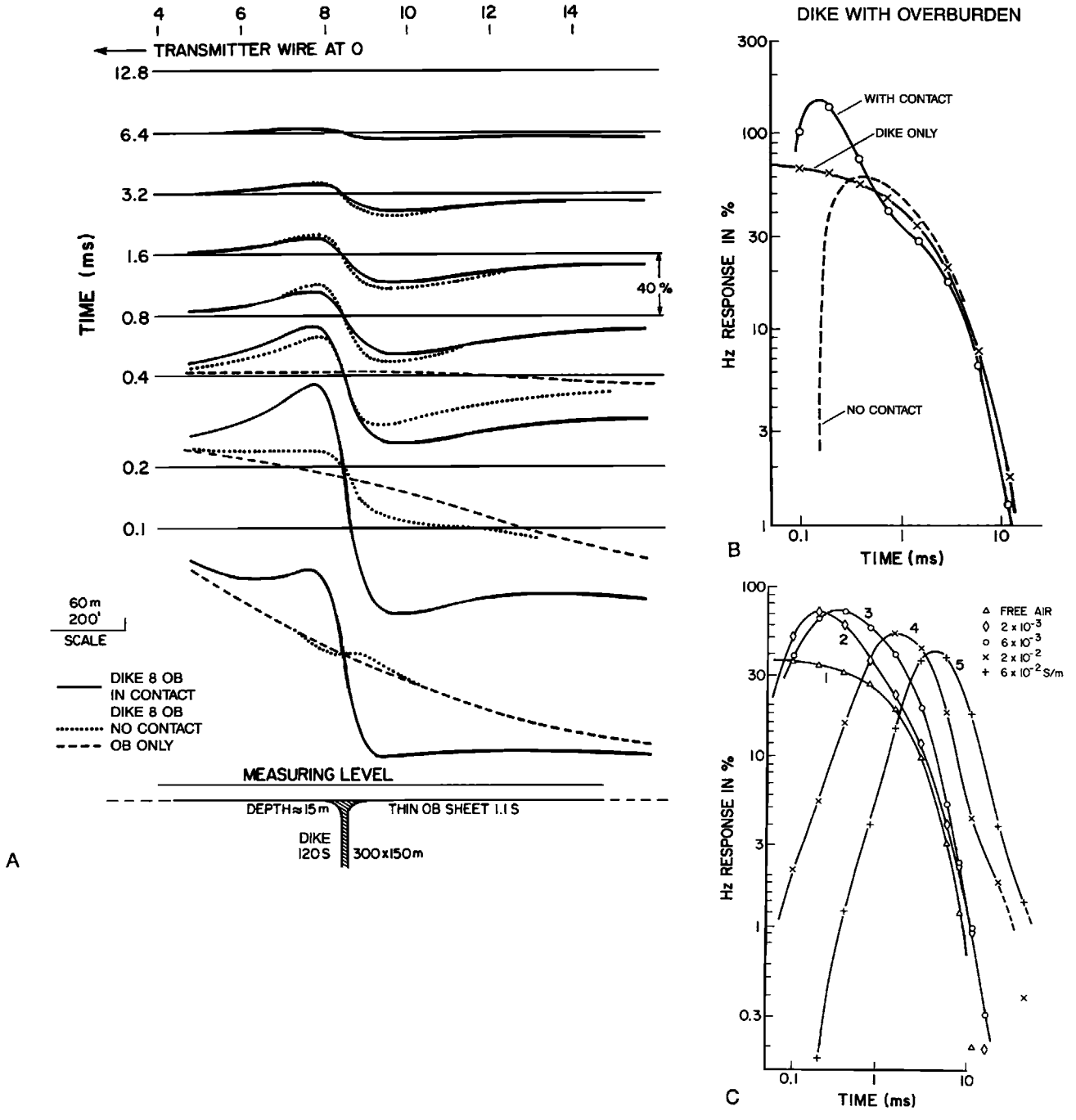

Fig. 32. (a) Time-domain step response from a scale model experiment similar to the model in Figure 31 (b) plotted decay characteristics and (c) decay plots of stripped response for a conductor in a half space obtained by Fourier transforming the curves in Figure 31 (after Lamontagne, 1975).

magnetic dipole in the body), G_{bt}^{Hm} (the horizontal magnetic field in the body due to a vertical magnetic dipole transmitter), and G_{rt}^{Hm} (the vertical magnetic field at the receiver due to the vertical magnetic dipole transmitter) can be evaluated from equation (21). The low frequency galvanic coupling terms G_{rb}^{Hj} (the vertical magnetic field at the receiver of the galvanic induced horizontal current dipole in the body) and G_{bt}^{Em} (the horizontal electric field in the body due to the vertical magnetic dipole transmitter) can be obtained from equations (72) and (74). Choosing $l = 2^{3/2} d$ which gives maximum coupling for vortex induction about a horizontal axis, and assuming a spherical conductor of radius a, we then obtain for the galvanic and vortex inductive terms of the secondary field anomaly

$$\frac{e^s}{e^p} = \frac{H^s}{H^p} = T_{oh}(\beta_{oh})\left\{\left[\frac{4\sqrt{2}}{27}\left(\frac{a}{d}\right)^3\left(\frac{\alpha}{1+\alpha}\right)i\beta_h\right] + \left[\frac{16\sqrt{2}}{27}\left(\frac{a}{d}\right)^3\left(\frac{i\gamma}{1+i\gamma}\right)\right]\right\}. \quad (80)$$

The result in equation (80) is just an example for one coil configuration, depth, and body shape. In this particular case, the inductive term dominates as long as the inductive time constant is large enough. Although N^g and $(1 - N^i)$ could be rather different in magnitude for a strongly ellipsoidal body, the obvious difference in the expressions is in their frequency dependence. The $i\beta_h$ in the galvanic response versus the $i\gamma/(1 + i\gamma)$ in the vortex inductive response generally ensures that, when the target body is a much better conductor than the host rock, frequencies can be found where the toroidal response will dominate the galvanic response. If the frequency is raised sufficiently above that necessary to reach the target body's inductive limit, the galvanic response should become dominant. However, if the overburden is much more conductive than the hostrock, all response from the target may be cutoff by the overburden transmission filter before that happens. The interrelationships are shown schematically in Figure 34.

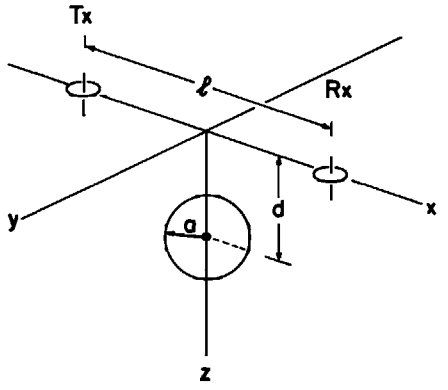

Fig. 33. Geometrical configuration for the case considered in equation (80).

TWO-DIMENSIONAL AND FAR-FIELD MODELS

Most of the foregoing has dealt with controlled source EM where the source is near the target body. If the zone of interest is in the far field of the source, or if the source field and the interesting conductivity structure are two-dimensional, there are several important differences.

A two-dimensional case is one in which the strike length, both of the structure and of the source field, is large compared both to the skin depth of the field in the host medium and to the important dimensions of the model in the principal cross-section. In such a case, the manner in which the actual structure and its exciting field terminate along strike has no effect on the observations, and this leads to great analytical simplifications. Unfortunately, it is rare in the interpretation of practical EM data when these criteria hold throughout the observed frequency spectrum. Only for the highest frequency data is the host skin depth likely to be sufficiently short.

In a far field case, the exciting field comes to the region of interest from a distant source through the air. The rate of falloff in the far zone is rapid in terms of fractional distance between the source and receiver, but because this distance is large compared to the dimensions of the region of interest and to the skin depth in the host medium, the lateral falloff in the intensity of the surface field across the zone of interest will be relatively small in comparison to the vertical attenuation (skin depth). If the ground is uniform laterally, the primary field in the region of interest will be nearly uniform laterally, at least over distances of a few skin depths in each direction. If the region considered in a model is a few skin depths in lateral and vertical dimensions, the primary field can be viewed as coming only from the top. However, if skin depth in the host material becomes large compared to the region of interest, the primary field must be considered as coming in from all sides of the model. The environment of the modeled structure will then have to be taken into account.

Two-dimensional modeling is attractive from a theoretical point of view because the EM field can then be separated rigorously into two species, TE (transverse electric) and TM (transverse magnetic) modes. Contrary to what a geologist might assume, "transverse" here indicates that the named field is in the strike direction. The separation enables us to write the EM

field equations in terms of two scalar variables which each satisfy completely independent equations. In the TE case, no charge distributions can form on conductivity contrasts because the electric field is always parallel to the interfaces. The distinction betwen galvanic and vortex induction then no longer exists. In a small conductive feature, the principal component of electromagnetic induction is a general unidirectional current flow along the body. Higher order terms involve flow in both directions. The principal term may be considered as a vortex induction closing at infinity or as a galvanic channeling current which enters the body at an infinite distance from the cross-sectional plane. The strength of such a current is not limited by external field self-induction or by depolarization, and the case mentioned in respect to equation (45) applies. The strength of the anomalous current in this case is limited only by skin effect in the current system. If the host medium is relatively insulating and the source is a nearby long wire, the secondary field has the usual resistive limit where the anomalous current is in quadrature phase with the source current and magnetic field and its strength is proportional to frequency. But as frequency is increased, the induc-

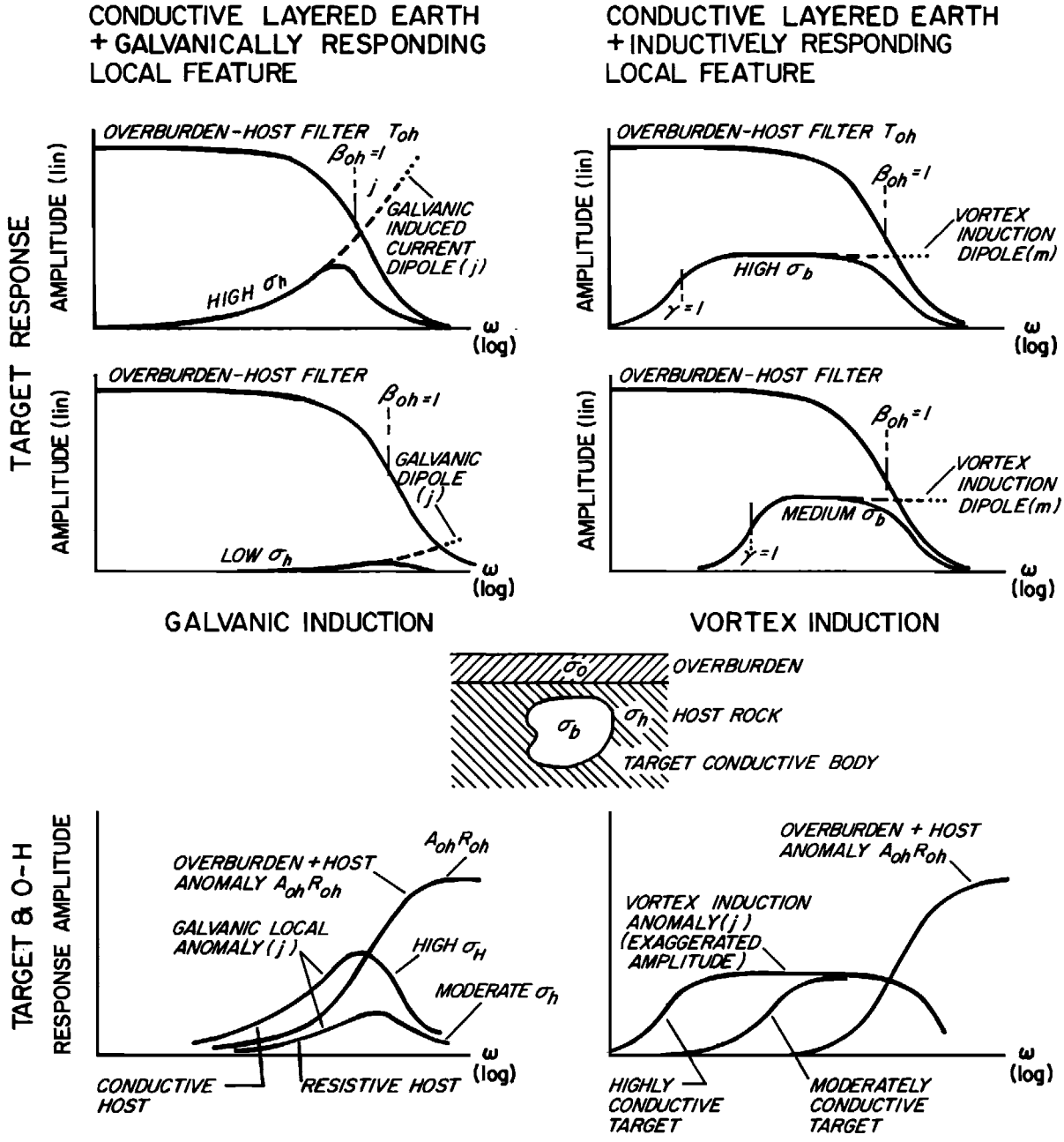

Fig. 34. Sketches of the frequency and time-domain response characteristics of galvanic and vortex induction.

tive limit is reached very slowly, with the phase angle remaining near 45 degrees, and the net amount of current flow along the target tending toward equality with the current in the source wire (but opposite in polarity). Unless the host medium is extremely resistive, its filtering effect on the primary and secondary fields will control the response before a full inductive limit is reached.

In TM modes, the direction of current flow is in the principal plane of the model, so charge distributions are created on conductivity boundaries. The physics of TM mode induction is therefore more similar to the three-dimensional, local source cases we have discussed. However, TM excitation of long strike conductive bodies is generally impractical or unfavorable from an EM prospecting point of view, so such models are of limited importance except for studying induction effects in resistivity and IP surveys, or in CSAMT where electric field measurement is a dominating factor.

Modeling of far-field EM prospecting methods such as VLF, E phase, AFMAG and magnetotellurics generally needs a different approach from that which is appropriate for near-field, controlled-source EM methods, and has not been considered here. The differences are most marked for modeling the response of large structures, where the scale of the significant induced current system is controlled by the skin depth of the host medium rather than by the size and configuration of the prospecting system. Induction in small targets with strong conductivity contrast to a uniform host medium (where "small" means small in comparison with host skin depth) is basically the same as described in the previous section except that the galvanic mechanism for generating anomalies is more important because the primary electric field is relatively strong. However, the background response from the overburden and host medium has a different form. Only the secondary field returning to the surface can be considered a localized field as discussed previously. The incident source field will obey a one-dimensional equation. It will generally be impractical to define primary field as the free space field of the source. A uniform or uniformly stratified half space excited from a distance will be the usual reference case.

EXPLORATION PHILOSOPHY

It is useful to consider two paradigms of EM exploration. The first has grown out of the search for massive sulphide base metal ores and is the conductor search problem. The object is to discover highly conductive regions within the ground, and at the same time obtain as much geometrical, dimensional, and conductivity information about them as possible. The problem is to maximize sensitivity to all significant conductors without obtaining too many false alarms from uninteresting geological features such as irregularities in conductive overburden, large moderately conductive bedrock formations such as graphitic metasediments, etc.

The second paradigm is three-dimensional mapping of ground structure. Here the objective is to map the three-dimensional conductivity structure of the ground in as much detail as possible without making strong prior assumptions about what the ground structure may be. In practice, due to the diffusive nature of the EM field, a highly simplified picture is all that can be obtained, even in the best of circumstances. The parameters of the EM measurement system will, in this case, be selected according to the depth range of interest and the anticipated range of earth conductivities in the investigated area. Any tuning of the system will be designed to maximize the information content of the EM system's data outputs over typical ground.

If searching for conductors is the objective, the logic developed in the conductive overburden and conductive host sections is applicable both in the design or selection of the EM system and in the interpretation of data. In choosing a system, we must first consider the ratio of target signal level to system noise level, and then devise means to combat the target to geologic noise problem. Basically, the transmitter moment, the physical scale and geometrical configuration of the EM coils, and frequency range all affect the EM system's ratio of target signal to system noise, and both scale and moment must be maximized for deep penetration. Naturally, geologic noise will be much more apparent in the data from deep penetration systems because of their very high sensitivity. Discrimination between prospective and nonprospective anomalies then becomes the key factor which limits performance. In the first instance, discrimination will likely be based on the observed time-constant(s) of the anomalous response. However, there may easily be a very significant overlap between the response time constant spectra of desirable targets and those of local structures in the host medium and overburden. Indeed, if the target responds galvanically, there will usually be little difference in spectral response of a bedrock target and an overburden structure. Various other means can then be used to effect discrimination but all are based in some way on geometry. With a wide band EM system of fixed transmitter-moving receiver type, the outward migration of the currents induced in the host-overburden structure can be tracked with time or frequency and separated from the relatively stationary response of local structures. The mechanism for generation of each local anomaly component can then be identified by model fitting. Much the same can be done with a moving source EM system, although identification of the two components may be somewhat more model

dependent. Ideally, of course, we would like to have broad band measurements made at each receiver station for several different distances and directions to the transmitter. In airborne systems, where the lateral separation of the receiver and transmitter is usually fixed and often small compared to flight height, differences in transmitter orientation can help with the discrimination problem.

It is our view that in any difficult EM exploration problem, stripping of response into separate components will usually be essential to making an interpretation. This process is not enhanced by plotting data on logarithmic amplitude scales or by transforming data to apparent resistivities. Nevertheless, a component of the response will usually be due to host-plus-overburden conductivity, and any interpretation of other components will require an estimate of the host-overburden structure as a starting point. Thus, an apparent resistivity (or apparent conductivity) approach to interpreting the regional structure can be fully justified. However, the physics involved in producing the rest of the response is usually not akin to the host-overburden induction problem, so local anomalies require a careful analysis. Free space induction models may be very appropriate for interpreting the stripped late time or low frequency response of a local conductive feature, even when strong galvanic response is likely in other parts of the response spectrum.

When three-dimensional mapping of conductivity structure is the objective, there is little alternative but to use a stratified earth model as the basic reference. If the EM survey is to provide a reasonably detailed, unambiguous interpretation, it must cover a wide enough frequency spectrum that skin depth in the important ground materials varies from much larger than the maximum depth of interest to a number that is small or at least comparable to the geometric mean of the EM system's scale size and the minimum depth of interest or required depth resolution. Whatever method is used, the soundings must be made with sufficient lateral density that the degree of lateral inhomogeneity in the ground can be determined in order that the suitability of a one-dimensional stratified earth interpretation model can be assessed. In a ground EM system with a separated transmitter and receiver, the spectral coverage should be sufficient that far-, active-, and near-zone response from the ground will be observed. The depth range explored by the induced currents will then shift from a value less than the receiver-transmitter coil separation (the minimum depth resolution) to one comparable to or substantially larger than the separation (the maximum depth of exploration). The high frequency far-zone data will reflect the conductivity of local surface structure near the receiver whereas the low frequency near-zone data (if such can be accurately observed) will reflect not only the deepest but also the most general aspects of the conductivity structure on a lateral scale larger than the receiver-transmitter separation.

In a conductivity mapping scenario, rapid spatial variation in response is much more likely to be due to the lateral heterogeneity of the typical conductors in the ground than due to zones of exceptionally high conductivity. Thus, it should be expected that most of the local anomalies will be of galvanic rather than vortex inductive type. Interpretation methods must take this into account.

REFERENCES

Annan, A. P., 1974, The equivalent source method for electromagnetic scattering analysis and its geophysical application: Ph.D. thesis, Memorial University of Newfoundland.

Eadie, E. T., 1979, Stratified earth interpretation using standard horizontal loop electromagnetic data, Research in applied geophysics no. 9, Geophys. Lab., Univ. of Toronto.

Edie, E. T., 1981, Detection of hydrocarbon accumulations by surface electrical methods: a feasibility study, Research in applied geophysics no. 15, Geophys. Lab., Univ. of Toronto.

Goldman, M. M. and Fitterman, D. V., 1987, Direct time-domain calculation of the transient response for a rectangular loop over a two-layer medium; Geophysics, **52**, 997–1006.

Grant, F. S. and West, G. F., 1965, Interpretation theory in applied geophysics: McGraw-Hill, New York.

Hanneson, J. E., and West, G. F., 1984, The horizontal loop electromagnetic response of a thin plate in a conductive earth: Geophysics, **49**, 411–420, (Part I), 421–432 (Part II).

Hohmann, G. W., 1988, Numerical modeling for electromagnetic methods in geophysics, *in* Nabighian, M. N., Ed., Electromagnetic methods in applied geophysics, Volume 1: Soc. Expl. Geophys., 313–363.

Holladay, J. S., 1981, YVESFT and CHANNEL: A subroutine package for stable transformation of sparse frequency domain electromagnetic data to the time domain: Research in applied geophysics, No. 17, Geophys. Lab., Dept. of Physics, Univ. of Toronto.

Kaufman, A. A., 1978, Frequency and transient responses of electromagnetic fields created by currents in confined conductors: Geophysics, **43**, 1002–1010.

Lajoie, J. J. and West, G. F., 1976, Electromagnetic response of a conductive inhomogeneity in a layered earth: Geophysics, **41**, 1133–1156.

Lamontagne, Y. L., 1975, Application of wideband, time-domain EM measurements in mineral exploration: Ph.D. thesis, Univ. of Toronto.

McNeill, J. D., Edwards, R. N., and Levy, G. M., 1984, Approximate calculations of the transient electromagnetic field from buried conductors in a conductive half-space: Geophysics, **49**, 918–933.

Nabighian, M. N., 1970, Quasi-static transient response of a conducting sphere in a dipolar field: Geophysics, **35**, 303–309.

Nabighian, M. N., 1971, Quasi-static transient response of a conducting permeable two-layer sphere in a dipolar field: Geophysics, **36**, 25–37.

Nabighian, M. N., 1979, Quasi-static transient response of a conducting half-space: An approximate representation: Geophysics, **44**, 1700–1705.

Smythe, W. R., 1968, Static and dynamic electricity, McGraw-Hill.
Wait, J. R., 1951a, A conducting sphere in a time varying magnetic field: Geophysics, **16**, 666–672.
Wait, J. R., 1951b, The magnetic dipole over the horizontally stratified earth: Canadian Journal of Physics, **29**, 577–592.
Ward, S. H. and Hohmann, G. W., 1988, Electromagnetic theory for geophysical applications, *in* Nabighian, M. N., Ed., Electromagnetic methods in applied geophysics, Vol. 1: Soc. Expl. Geophys., 131–312.
Weidelt, P., 1983, The harmonic and transient electromagnetic response of a thin dipping dike: Geophysics, **48**, 934–952.
West, G. F., Macnae, J. C., and Lamontagne, Y., 1984, A time-domain electromagnetic system measuring the step response of the ground: Geophysics, **49**, 1010–1021.
West, G. F., and Edwards, R. N., 1985, A simple parametric model for the elctromagnetic response of an anomalous body in a host medium, Geophyscs, **50**, 242–257.